

# 扬子西缘荣经地区三叠纪碎屑物源分析

张英利<sup>1)</sup>, 贾晓彤<sup>2)</sup>, 王坤明<sup>1)</sup>, 王宗起<sup>1)</sup>, 陈木银<sup>3)</sup>

1) 中国地质科学院矿产资源研究所自然资源部成矿作用与资源评价

重点实验室, 北京, 100037;

2) 浙江省地震局信息中心(应急服务中心), 杭州, 310013;

3) 中国石油集团测井有限公司长庆事业部, 西安, 710201



www.  
geojournals.cn/georev

**内容提要:** 扬子西缘早三叠世处于伸展环境, 而晚三叠世为前陆盆地。扬子西缘三叠系保存较好, 是研究三叠纪构造转换物源响应方面的理想场所。本文根据重矿物电子探针和碎屑锆石测年, 分析三叠系的物质来源, 进而探讨与构造环境的对应关系。电气石探针结果显示, 下三叠统主要源自贫锂花岗岩类伴生伟晶岩和细晶岩、变质板岩、变质砂岩、钙质硅酸盐岩和电气石石英岩, 上三叠统主要来自贫锂花岗岩类伴生伟晶岩和细晶岩、贫钙变质板岩、变质砂岩和电气石石英岩, 且自下三叠统至上三叠统变板岩和变砂岩的物源区比重逐渐增加; 尖晶石显示, 下三叠统砂岩主要来自大火成岩省、洋岛玄武岩和岛弧玄武岩类, 上三叠统主要来自岛弧玄武岩类。碎屑锆石 U-Pb 测年结果表明, 早三叠世碎屑锆石峰值为 251~265 Ma、460~535 Ma 和 544~987 Ma, 晚三叠世碎屑锆石峰值为 228~251 Ma、255~387 Ma、429~523 Ma、573~954 Ma、1720~2004 Ma 和 2453~2494 Ma。综合分析表明, 下三叠统沉积物主要来自峨眉山玄武岩、康滇古陆, 少量来自南秦岭造山带, 而上三叠统的物源区主要为峨眉山玄武岩、康滇古陆、秦岭造山带和华北板块。三叠系物源的差异, 主要与晚三叠世秦岭造山带与扬子板块碰撞有关。

**关键词:** 物源分析; 重矿物电子探针; 碎屑锆石年代学; 三叠纪; 扬子克拉通西缘

扬子西缘作为扬子陆块的重要组成部分, 经历新元古代和古生代的多期构造运动 (Xu Yigang et al., 2004; Dong Yunpeng et al., 2012; Zhu Min et al., 2017), 直至晚三叠世印支造山运动之后 (Deng Tao et al., 2019; Yan Zhaokun et al., 2019), 形成目前的构造格局。三叠纪时期, 早—中三叠世为伸展环境, 而晚三叠世为挤压环境——前陆盆地 (戴朝成等, 2014; Deng Tao et al., 2019; Yan Zhaokun et al., 2019)。三叠系的研究主要集中于沉积岩相古地理 (林文球等, 1982; 王正瑛和邓江红, 1982; 曹剑等, 2004; Xu Chunming et al., 2015; 张英利等, 2019) 和晚三叠世构造环境 (戴朝成等, 2014; 陈斌等, 2016; Deng Tao et al., 2019; Yan Zhaokun et al., 2019) 等。然而, 三叠纪构造转换相关的沉积物源等特征仍存在不同观点。对于下三叠统物源区的系统研究相对薄弱。重矿物和碎屑锆石 U-Pb 测年结果的物源分析表明, 会泽地区下三叠统主要来自于

康滇古陆 (张英利等, 2016)。上三叠统的物源分析研究较多, 认为是前陆盆地沉积记录的响应, 但物源区争议较多。Zhu Min 等 (2017) 和 Yan Zhaokun 等 (2019) 的碎屑锆石 U-Pb 年龄结果, 表明晚三叠世康滇古陆与西部义墩岛弧连接在一起, 隆升形成较大范围的康滇古陆, 成为重要的物源区。除此之外, 华北板块也是重要的物源区 (Zhang Yong et al., 2015; Yan Zhaokun et al., 2019)。Tan Xiucheng 等 (2013) 根据层序地层学表明上三叠统物源来自于西部松潘—甘孜造山带; 戴朝成等 (2014) 根据碎屑组成和岩相古地理, 表明研究区物源主要来自西南峨眉瓦山古陆。Mu Hongxu 等 (2019) 根据龙门山钻井剖面对比、岩相古地理, 辅助碎屑锆石 U-Pb 测年, 表明研究区北侧的须家河组的物源主要来自于秦岭造山带。然而, 须家河组砂岩的地球化学分析表明, 须家河组物源区除西北龙门山造山带之外, 部分来自于川东南的龙泉山前陆隆起冲带 (Yang Wei

注: 本文为深地资源勘查开采项目(编号:2019YFC0605202), 国家自然科学基金资助项目(编号:41302080)和中国地质调查局项目(编号:DD20201173)的成果。

收稿日期: 2020-12-07; 改回日期: 2021-04-12; 责任编辑: 赵雪、章雨旭。Doi: 10.16509/j.georeview.2021.04.123

作者简介: 张英利, 男, 1979 年生; 正高级工程师, 主要从事沉积学与盆地构造研究; Email: yinglizh@126.com。

et al., 2019)。须家河组黑色泥岩的地球化学分析结果显示,须家河组一段源自秦岭造山带元古代和早古生代地层,须家河组三段源自龙门山新元古代杂岩,而须家河组五段源自松潘—甘孜复理石地层 (Deng Tao et al., 2019)。因此,三叠系物源特征分歧很大,即物源区包括龙门山造山带、秦岭造山带、松潘—甘孜造山带、康滇古陆、川东南构造带等等,这些不同观点严重阻碍区域演化的认识。而且,采用单一方法确定物源区存在局限性 (Armstrong-Altrin and Verma, 2005; Moecher and Samson, 2006)。

重矿物是物源分析的重要手段,尤其是电气石、尖晶石、碎屑锆石等,能够很好地反映物源区母岩类型 (Kamenetsky et al., 2001; von Eynatten and Dunkl, 2012; 姜磊等, 2019)。多种重矿物的综合分析可以定量、定性反映物源区岩石类型和岩石形成年龄以及物源区岩石形成的构造背景,为源区母岩的确定提供综合依据。

本文选择龙门山构造带和康滇古陆结合部的荥经作为研究区,对三叠纪样品分别开展碎屑重矿物电子探针和碎屑锆石测年工作,确定不同地层的物源区母岩和物源区,进而阐述沉积物源与不同构造体制的对应关系。

## 1 地质背景

扬子陆块周缘以深大断裂为界由不同构造单元组成,北邻碧口地块(南秦岭造山带的一部分),西邻松潘—甘孜造山带、哀牢山构造带和思茅地块。碧口地块主要由碧口群、横丹群和鱼洞子群及古元古代—新元古代镁铁质侵入岩和中酸性侵入岩组成,碧口群为火山熔岩、火山碎屑岩等,横丹群主要为变火山沉积岩,鱼洞子群为斜长角闪岩、浅粒岩夹磁铁石英岩等。以碧口地块等组成的南秦岭造山带,前寒武纪多经历洋壳俯冲—弧陆碰撞 (Wang Wei et al., 2012; Dong Yunpeng et al., 2012)。古生代以商丹(商南—丹凤)缝合带和勉略(勉县—略阳)缝合带为界,秦岭造山带经历复杂的造山作用,形成不同的构造单元,发育大量岩浆岩(王宗起等, 2009; Dong Yunpeng et al., 2016)。晚三叠世南秦岭造山带与扬子板块碰撞 (Yin An and Nie Shangyou, 1993; Meng Qingren et al., 1999, 2005), 形成前陆盆地。松潘—甘孜造山带二叠纪—三叠纪主体受古特提斯大洋影响,发育增生楔杂岩和增生岛弧,局部残存古特提斯大洋盆地及被构造移置的洋壳残片,中三叠世拉丁期受西秦岭岛弧地体与扬子陆块碰撞影

响,形成周缘前陆盆地(夏磊等, 2017),三叠纪整体沉积厚层浊积岩。哀牢山构造带和思茅地块作为三江造山带的重要组成部分,在前特提斯时期亲扬子地块。晚古生代—早中生代古特提斯洋打开之后,与扬子板块分化成 2 个属性不同的构造单元(刘俊来等, 2011)。早石炭世一二叠纪,哀牢山洋盆俯冲,形成哀牢山构造带(由混杂岩和岛弧类岩石组成)和思茅弧后盆地。早三叠世哀牢山构造带和思茅地块隆升遭受剥蚀,中一晚三叠世与扬子陆块碰撞,形成弧后前陆盆地(谭富文等, 2001; 杨鑫等, 2010)。扬子板块东南的雪峰造山带晚三叠世隆升 (Yan Danping et al., 2003; 田洋等, 2015), 成为扬子东南缘沉积物的重要源区。

古生代早期,上扬子地区相对较稳定,处于克拉通演化阶段(黄福喜等, 2011; 陈洪德等, 2011)。晚二叠世包括研究区在内的上扬子地区受地幔柱作用,发育峨眉山大火成岩省 (Xu Yigang et al., 2004; 宋谢炎等, 1999; Hei Huixin et al., 2018)。受峨眉山玄武岩影响,晚二叠世宣威组形成于裂谷环境 (Zhang Yingli et al., 2019)。早—中三叠世,扬子西缘处于伸展环境(陈洪德等, 2011; 张英利等, 2019)。晚三叠世,秦岭造山带和扬子陆块经历碰撞造山运动,发育以须家河组沉积物为代表的前陆盆地(郑荣才等, 2012; Zhang Yong et al., 2015; Yan Zhaokun et al., 2019)。

研究区位于荥经地区,临近龙门山断裂和小江断裂交汇处(图 1a)。研究区周缘主要发育北东向逆断裂,少量断裂为北西向。断层上盘出露新元古代花岗岩和辉绿岩、新元古代火山碎屑岩—碳酸盐岩以及早古生代碎屑岩—碳酸盐岩(图 1b)。距研究区北西约 50 km 的天全花岗岩年龄为  $851 \pm 15$  Ma (赖绍聪等, 2015)。新元古代火山碎屑岩—碳酸盐岩主要由震旦系苏雄组和灯影组构成。苏雄组主要为凝灰岩、流纹岩与火山角砾岩等,区域上获得地层年龄为 780~838 Ma (Li Xianhua et al., 2002; 卓皆文等, 2017)。灯影组主要为白云岩和硅质白云岩,局部夹凝灰岩,凝灰岩年龄约 539 Ma (资金平等, 2017)。寒武系—志留系主要为白云岩、石英砂岩、生物碎屑灰岩和泥岩。断层下盘为上二叠统峨眉山玄武岩和宣威组、下三叠统飞仙关组、嘉陵江组和上三叠统须家河组以及侏罗系。上二叠统峨眉山玄武岩主要由玄武岩、流纹岩等组成,年龄为 258~254 Ma (Xu Yigang et al., 2004),宣威组与峨眉山玄武岩同期异相,主要为陆源碎屑岩 (Zhang Yingli et

al., 2019)。下三叠统飞仙关组主要为暗紫色、紫红色中层细砂岩夹粉砂岩和泥岩,粉砂岩和泥岩发育水平层理。区域上,沉积环境为冲积扇—河流—潮坪(林文球等,1982;张英利等,2016)。嘉陵江组主要为灰色碎屑岩和灰色灰岩,沉积环境为潮坪—潟湖(林文球等,1982;张英利等,2019)。中三叠统雷口坡组在研究区不发育,但在研究区南部30 km出露,主要为灰色细砂岩夹泥质白云岩及泥岩。上三叠统须家河组为河流和湖泊沉积的陆源碎屑岩(郑荣才等,2012;Deng Tao et al., 2019; Yan Zhaokun et al., 2019),下部为灰色、深灰色厚层细砂岩夹粉砂岩、泥岩及可采煤,中部为灰色、深灰色厚层泥质粉砂岩、粉砂质泥岩,局部夹煤线,上部为浅灰色厚层细砂岩与薄层粉砂质泥岩互层。

## 2 样品采集和测试方法

本次研究采取荣经花滩镇冯家坝至斑鸠井煤矿路线三叠系细砂岩样品(图1b),其中飞仙关组样品(HT1)的坐标为 $29^{\circ}49'32''$ , $102^{\circ}44'39''$ 。须家河组

样品(HT8)的坐标为 $29^{\circ}52'09''$ , $102^{\circ}43'56''$ 。每件样品采集约10 kg。样品经过粉碎、筛选和分离后,在双目镜下挑选电气石、尖晶石和锆石单矿物。每种矿物选出至少500粒,便于开展电子探针和碎屑锆石测年分析。

### 2.1 电子探针

电子探针测试在中国地质大学(北京)电子探针实验室完成,仪器型号为日本岛津公司生产的EPMA-1600。测试条件为加速电压15 kV,激发电流10 nA,电子束直径1  $\mu\text{m}$ ,ZAF法修正。分析标样采用磁铁矿(Fe)、钠长石(Si、Na、Al)、磷灰石(Ca、P)、金红石(Ti)、蔷薇辉石(Mn)、透长石(K)、橄榄石(Mg)、萤石(F)、独居石(La、Ce、Pr、Nd、Th)、锆石(Y、Zr、Hf)、铯榴石(Rb、Cs)、单矿物(U、Ta、Nb)等。主元素(含量高于>20%)的允许的相对误差≤5%,含量在3%~20%之间的元素允许的相对误差≤10%,含量在1%~3%的元素允许的相对误差≤30%,而含量在0.5%~1%之间的元素允许的相对误差<50%。基于31个氧原子,对电子探针分析的

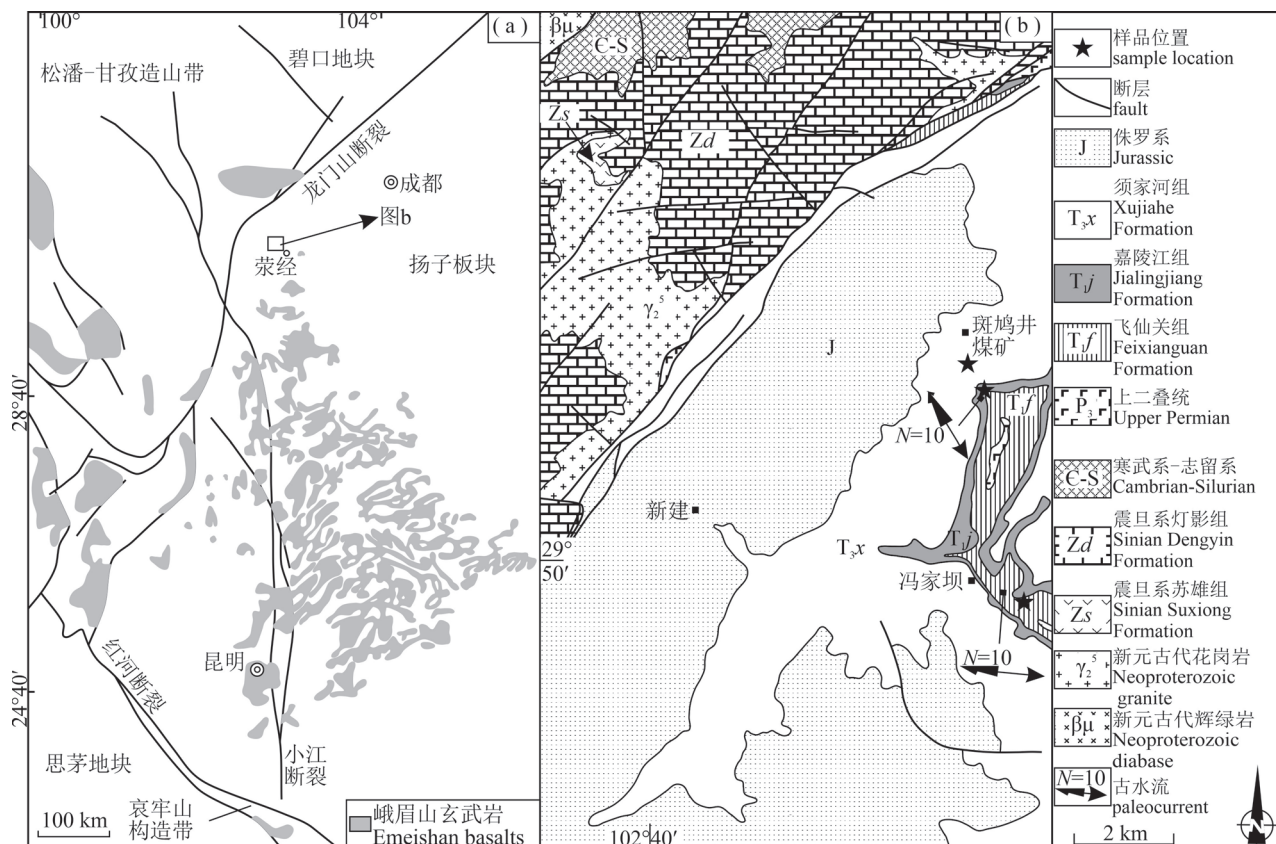


图1 扬子西缘大地构造单元图(a,据 Xu Yigang et al., 2004)和荣经地区地质图(b,据1:5万新建幅和泗坪幅地质图修改)

Fig. 1 Tectonic units of the western margin of the Yangtze Craton (a, modified after Xu Yigang et al., 2004) and geological sketch map of Yingjing area (b, from 1:50000 Regional Geological Report of Xinjian and Siping area)

电气石数据进行处理(附表 1, 印刷版略, 请见电子版 [www.geojournals.cn/georev](http://www.geojournals.cn/georev))。铬尖晶石数据采用 CALCMIN excel 程序(Brandelik, 2009)进行处理(附表 2, 印刷版略, 请见电子版 [www.geojournals.cn/georev](http://www.geojournals.cn/georev))。

## 2.2 碎屑锆石

锆石样品的制靶工作和阴极发光图像由中国地质科学院地质研究所大陆动力学实验室完成。碎屑锆石的 U-Pb 年龄测定前, 根据透射光、反射光和阴极发光图像分析, 随机圈定裂隙不发育的颗粒。LA-ICP-MS 锆石测年分析在中国地质科学院矿产资源研究所自然资源部成矿规律与成矿评价重点实验室完成, 实验过程和步骤见侯可军等(2009)。数据

处理采用 ICPMSDataCal 程序(Liu Yongsheng et al., 2010), 普通 Pb 校正采用 Anderson(2002)方法。对于锆石年龄  $> 1000$  Ma 的数据, 采用  $n(^{207}\text{Pb})/n(^{206}\text{Pb})$  年龄, 而对于  $< 1000$  Ma 的数据, 采用  $n(^{206}\text{Pb})/n(^{238}\text{U})$  年龄(Gehrels et al., 1999; Sircombe, 1999)。谐和度 90%~110% 的数据为有效数据(附表 3, 印刷版略, 请见电子版 [www.geojournals.cn/georev](http://www.geojournals.cn/georev))。锆石年龄谐和图等采用 Isoplot 3.0 程序完成(Ludwig, 2003)。

## 3 测试结果

### 3.1 电气石电子探针

显微照片显示, 飞仙关组样品 HT1 电气石主要

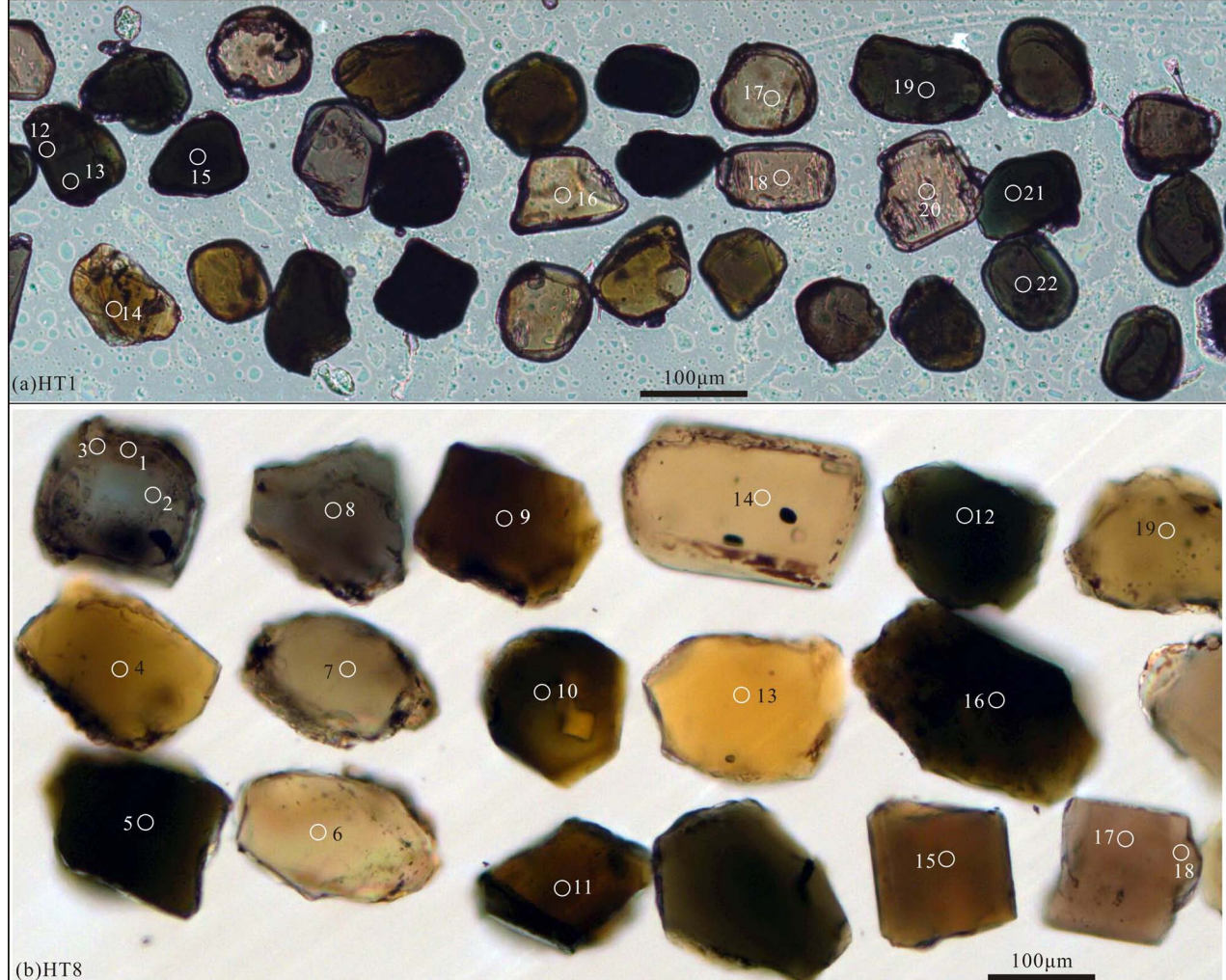


图 2 扬子克拉通西缘下三叠统飞仙关组(a)和上三叠统须家河组(b)砂岩电气石透射光图像

Fig. 2 Photomicrographs features of representative detrital tourmalines from sandstones of the Lower Triassic Feixianguan Formation (a) and the Upper Triassic Xujiahe Formation (b) on the western margin of the Yangtze Craton

○代表探针位置, 数字为点号

○—location, number—spot No.

为黑色、褐色、浅黄色,而须家河组样品 HT8 电气石主要为褐色、浅黄色和灰绿色(图 2),表明飞仙关组和须家河组物源存在差异。背散射图像显示,多数电气石呈均质、无环带。大多数电气石颗粒为次圆状和圆状,样品 HT1 颗粒较小(0.06~0.12 mm),样品 HT8 粒径主要介于 0.13~0.25 mm(图 2)。

样品 HT1 电气石颗粒的  $\text{SiO}_2$  含量为 32.72%~37.56%,  $\text{Al}_2\text{O}_3$  含量为 25.25%~35.32%, 而  $\text{B}_2\text{O}_3$  含量为 9.91%~10.84%。样品 HT8 电气石颗粒的  $\text{SiO}_2$  含量 33.97%~37.89%,  $\text{Al}_2\text{O}_3$  含量介于 25.00%~34.17%, 而  $\text{B}_2\text{O}_3$  含量为 10.33%~10.99%。基于 Henry 等(2011)的电气石分类图解,样品 HT1 除各 1 个数据点分别落于钙性系列和 X 空位系列之外,其余所有电气石均属于碱性类型,而样品 HT8 所有电气石均属于碱性类型(图 3a)。在  $n(\text{Mg})/[n(\text{Mg})+n(\text{Fe})]$  vs.  $\gamma/[\gamma+n(\text{Na})+n(\text{K})]$  阳离子数比值图解中(图 3b),样品 HT1 除了 1 个数据点落入镁铁电气石区域外,其余数据点落在黑电气石—镁电气石区域,且黑电气石与镁电气石个数比为 15:4;样品 HT8 数据点全部落在黑电气石—镁电气石区域(图 3b),且黑电气石与镁电气石个数比为 13:20。嘉陵江组样品(HT5)与 HT1 特征

类似。

在 Al—Fe—Mg 三角图(图 4a),下三叠统样品 HT1 和 HT5 电气石主要落于 2、4、5、6 区域,指示物源主要来自于贫锂花岗岩类及其关联的伟晶岩和细晶岩、富铁电气石岩石(蚀变花岗岩)、变质板岩和变质砂岩及富铁电气石石英岩、钙质硅酸盐岩和变质板岩。上三叠统样品 HT8 电气石主要落于 2、4、5 区域(图 4a),指示物源主要来自于贫锂花岗岩类及其关联的伟晶岩和细晶岩、富铁电气石岩石(蚀变花岗岩)、变质板岩和变质砂岩。在 Ca—Fe—Mg 三角图(图 4b),下三叠统样品 HT1 和 HT5 电气石主要落入贫锂花岗岩类伴生伟晶岩和细晶岩、贫钙变质板岩、变质砂岩和电气石石英岩区域,个别落入富钙变质板岩、变质砂岩和钙质硅酸盐岩区域,上三叠统样品 HT8 电气石主要落入贫锂花岗岩类伴生伟晶岩和细晶岩、贫钙变质板岩、变质砂岩和电气石石英岩区域。

### 3.2 铬尖晶石电子探针

下三叠统飞仙关组和上三叠统须家河组砂岩中碎屑铬尖晶石 BSE 图像显示,颗粒多呈次棱角状—次圆状,表明经历搬运、再旋回沉积。铬尖晶石数据表明,飞仙关组  $\text{Cr}^{\#}$   $\left[ \text{Cr}^{\#} = \frac{100 n(\text{Cr})}{n(\text{Cr}) + n(\text{Al})} \right]$  为 57~81,

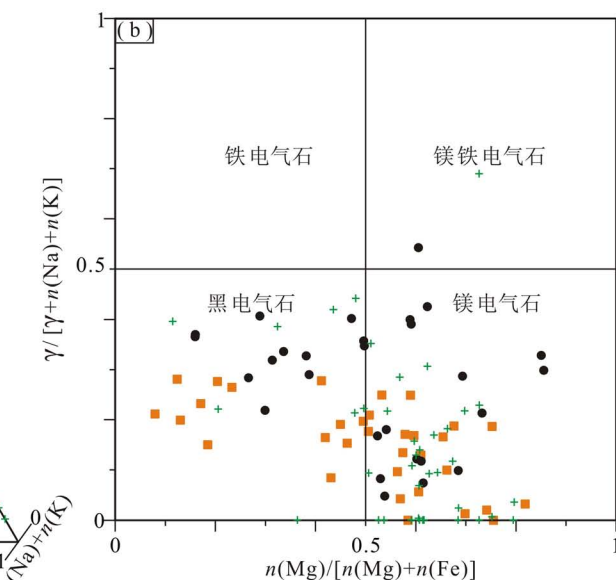
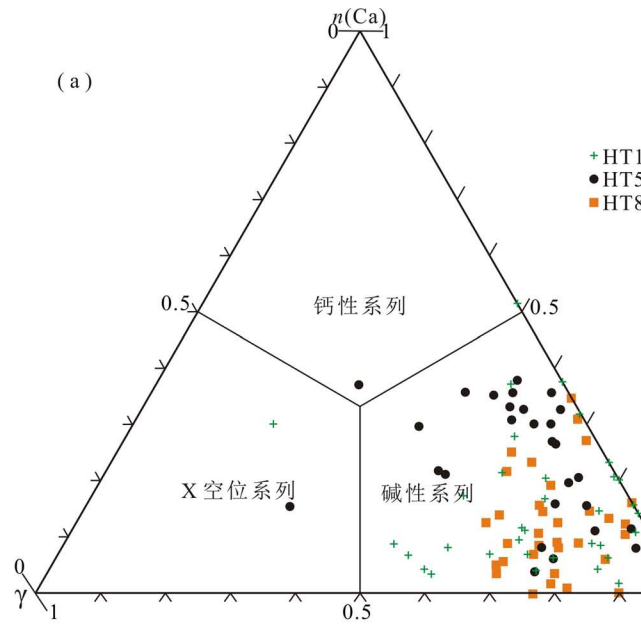


图 3 扬子克拉通西缘三叠系碎屑电气石阳离子  $n(\text{Ca})-\gamma-[n(\text{Na})+n(\text{K})]$  三元分类(a)和  $n(\text{Mg})/[n(\text{Mg})+n(\text{Fe})]$  vs.  $\gamma/[\gamma+n(\text{Na})+n(\text{K})]$  阳离子数比值图(b)(底图据 Henry et al., 2011, HT5 数据引自张英利等, 2019)

Fig. 3 The  $n(\text{Ca})-\gamma-[n(\text{Na})+n(\text{K})]$  ternary diagram (a) and  $\gamma/[\gamma+n(\text{Na})+n(\text{K})]$  vs.  $n(\text{Mg})/[n(\text{Mg})+n(\text{Fe})]$  diagram (b) of the detrital tourmalines from the Triassic sandstones on the western margin of the Yangtze Craton (after Henry et al., 2011; data of HT5 from Zhang Yingli et al., 2019&)

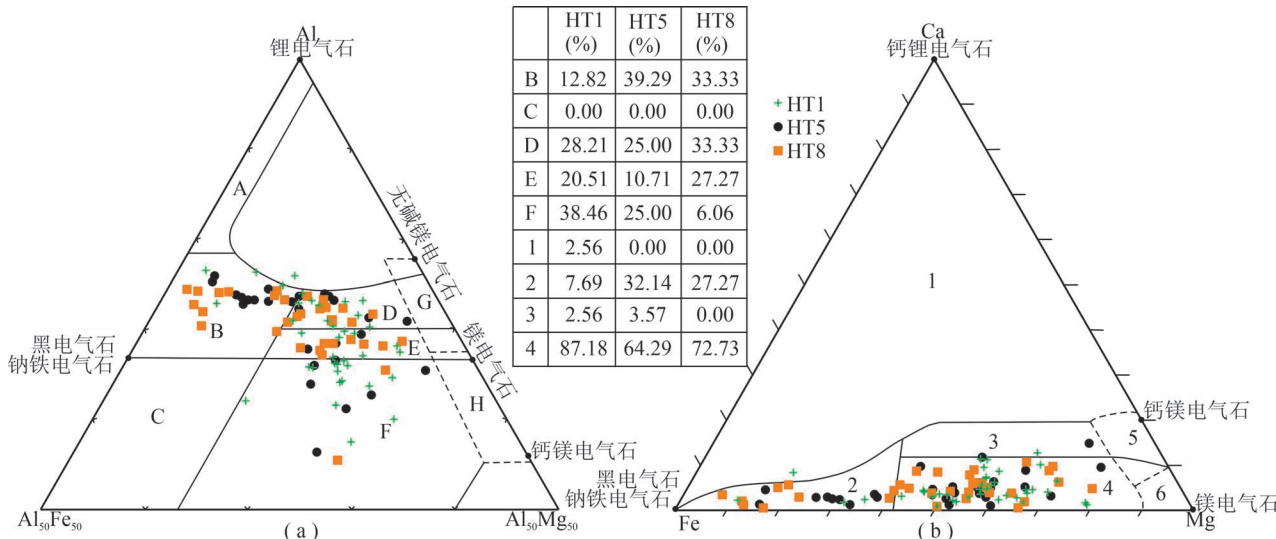


图 4 扬子克拉通西缘三叠系砂岩碎屑电气石的物源成分划分图解: (a) Al—Fe—Mg 图解; (b) Ca—Fe—Mg 图解  
(底图据 Henry and Guidotti, 1985; HT5 数据引自张英利等, 2019)

Fig. 4 Composition of the detrital tourmalines from the Triassic sandstones on the western margin of Yangtze Craton plotted on the ternary classification diagrams: (a) Al—Fe—Mg diagram; (b) Ca—Fe—Mg diagram (after Henry and Guidotti, 1985; data of HT5 from Zhang Yingli et al., 2019&)

1—富锂花岗岩、伟晶岩和细晶岩;2—贫锂花岗岩类及其关联的伟晶岩和细晶岩;3—富铁电气石岩石(蚀变花岗岩);4—伴生铝饱和相共存的变质板岩和变质砂岩;5—不伴生铝饱和相的变质板岩和变质砂岩;6—富铁电气石石英岩、钙质硅酸盐岩和变质板岩;7—低钙变超基性岩和富铬、钒变沉积岩;8—变碳酸盐岩和变质辉岩。9—富钙变质板岩、变质砂岩和钙质硅酸盐岩;10—贫钙变质板岩、变质砂岩和电气石英岩;11—变质碳酸盐岩;12—变超基性岩

1—Li-rich granitoid, pegmatites and aplites; 2—Li-poor granitoids and their associated pegmatites and aplites; 3—Fe-rich tourmaline rocks (hydrothermally altered granites); 4—metapelites and metapsammites coexisting with an Al-saturating phase; 5—metapelites and metapsammites not coexisting with an Al-saturating phase; 6—Fe-rich quartz—tourmaline rocks, calc-silicate rocks, and metapelites; 7—low-Ca meta-ultramafics and Cr, V-rich metasediments; 8—metacarbonates and metapyroxenites; 9—Ca-rich metapelites, metapsammites, and calc-silicate rocks; 10—Ca-poor metapelites, metapsammites, and quartz—tourmaline rocks; 11—metacarbonates; 12—metaultramafic rocks

平均 72;须家河组  $\text{Cr}^{\#}$  为 48~92, 平均 73。飞仙关组

$\text{Mg}^{\#}$   $\left[ \text{Mg}^{\#} = \frac{100 n(\text{Mg})}{n(\text{Mg}) + n(\text{Fe})} \right]$  为 21~53, 平均 43; 须家

河组  $\text{Mg}^{\#}$  为 15~65, 平均 40(附表 2)。 $\text{Cr}^{\#}$ — $\text{Mg}^{\#}$  指示, 飞仙关组尖晶石为铬铁矿和镁铬铁矿; 须家河组尖晶石主要为铬铁矿, 少量为镁铬铁矿, 个别为尖晶石和铁尖晶石。因此, 须家河组的物源与飞仙关组有所不同。

根据  $\text{TiO}_2$  的含量, 三叠系砂岩中尖晶石几乎全是火山岩成因。 $\text{Al}_2\text{O}_3$ — $\text{TiO}_2$  图解显示(图 5a), 下三叠统飞仙关组主要来自大火成岩省和洋岛玄武岩类岩石, 而上三叠统须家河组主要来自岛弧类岩石, 少量来自洋岛玄武岩类岩石。且  $n(\text{Cr})/[n(\text{Cr}) + n(\text{Al})]$ — $\text{TiO}_2$  图解(图 5b)表明, 下三叠统飞仙关组主要是板内玄武岩, 而上三叠统须家河组主要是岛弧玄武岩(图 5)。 $\text{Fe}^{3+}$ — $\text{Cr}^{3+}$ — $\text{Al}^{3+}$  图解, 下三叠

统飞仙关组较集中, 而上三叠统须家河组相对分散, 在岛弧玄武岩、洋岛玄武岩、大陆溢流玄武岩的叠合区域(图 5c)。

### 3.3 碎屑锆石

下三叠统飞仙关组样品 HT1 的碎屑锆石呈半自形、他形结构, 大部分锆石呈无色透明, 少数为玫瑰色。CL 图像显示, 颗粒大多数呈弱振荡环带(图 6a)。锆石粒径大小介于 80~200  $\mu\text{m}$ 。U-Pb 年龄值变化于  $251 \pm 2$  Ma~ $2528 \pm 11$  Ma, 主要集中于 251~265 Ma、460~535 Ma 和 544~987 Ma 区间(图 7b)。

上三叠统须家河组样品 HT8 碎屑锆石呈半自形结构, CL 图像显示颗粒大多数呈振荡环带(图 6b)。锆石粒径大小介于 80~240  $\mu\text{m}$ 。U-Pb 年龄值变化于  $238 \pm 3$ ~ $2653 \pm 9$  Ma, 主要集中于 228~251 Ma、255~387 Ma、429~523 Ma、573~954 Ma、1720~

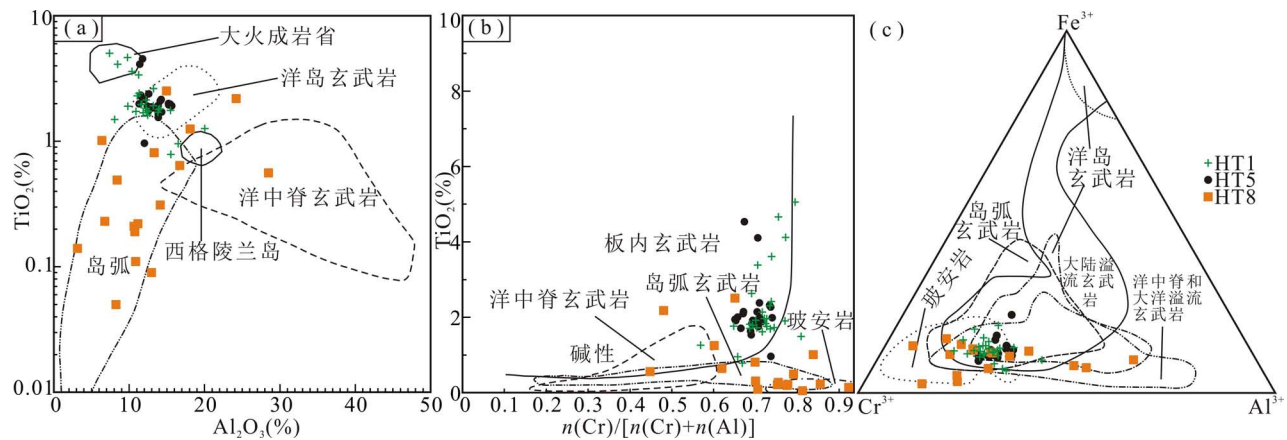


图5 扬子克拉通西缘砂岩碎屑铬尖晶石电子探针图解: (a)  $\text{TiO}_2$ — $\text{Al}_2\text{O}_3$  图解(据 Kamenetsky et al., 2001); (b)  $\text{TiO}_2$ — $n(\text{Cr})/[n(\text{Cr})+n(\text{Al})]$  图解(据 Arai, 1992); (c)  $\text{Fe}^{3+}$ — $\text{Cr}^{3+}$ — $\text{Al}^{3+}$  图解(据 Barnes et al., 2001)。HT5 数据引自张英利等, 2019

Fig. 5 The composition discrimination diagrams of the detrital chromian spinels from the Triassic sandstones on the western margin of the Yangtze Craton: (a)  $\text{TiO}_2$ — $\text{Al}_2\text{O}_3$  diagram ( after Kamenetsky et al. , 2001); (b)  $\text{TiO}_2$ — $n(\text{Cr})/[ n(\text{Cr}) + n(\text{Al}) ]$  diagram ( after Arai, 1992); (c)  $\text{Fe}^{3+}$ — $\text{Cr}^{3+}$ — $\text{Al}^{3+}$  diagram ( after Barnes et al. , 2001). Data of HT5 are adopted from Zhang Yingli et al. (2019&)

2004 Ma 和 2453~2494 Ma(图 7d)。

## 4 讨论

扬子西缘造山带较多,都可能成为三叠系的物源区。因松潘—甘孜造山带三叠系发育浊积岩(夏磊等,2017),不能成为扬子西缘的物源区。三江造山带位于研究区西南,岩相古地理显示(崔可信,2004;马永生,2009;Li Yingqiang et al., 2021),三叠

纪康滇古陆已经隆起,阻挡了三江造山带的沉积物搬运至研究区,因此,三江造山带不可能作为扬子西缘的物源区。雪峰造山带位于研究区东南,晚三叠世时期,雪峰造山带作为物源区为川东南的须家河组提供了沉积物源,而荣经地区须家河组的物源方向和沉积相的时空展布(崔可信,2004;马永生,2009)表明,荣经地区的沉积物源来自于西部或西北,因此,排除雪峰造山带作为物源区。

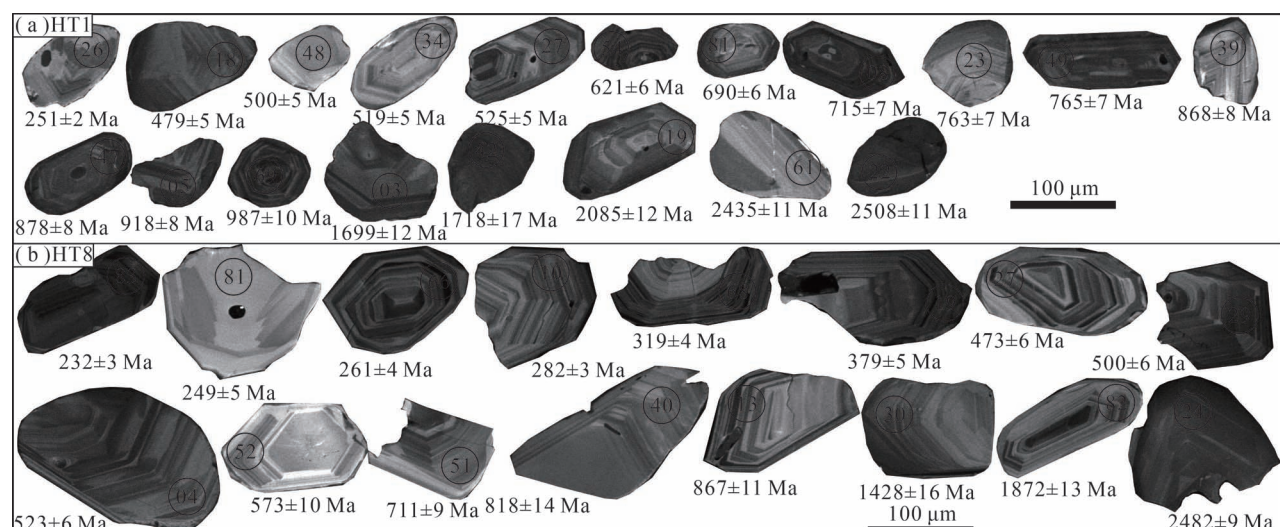


图6 扬子克拉通西缘下三叠统飞仙关组(a)和上三叠统须家河组(b)砂岩碎屑锆石阴极发光图像

Fig. 6 Cathodoluminescence (CL) images of representative zircons from the sandstones of the Lower Triassic Feixianguan Formation ( a ) and the Upper Triassic Xujiahe Formation ( b ) on the western margin of the Yangtze Craton

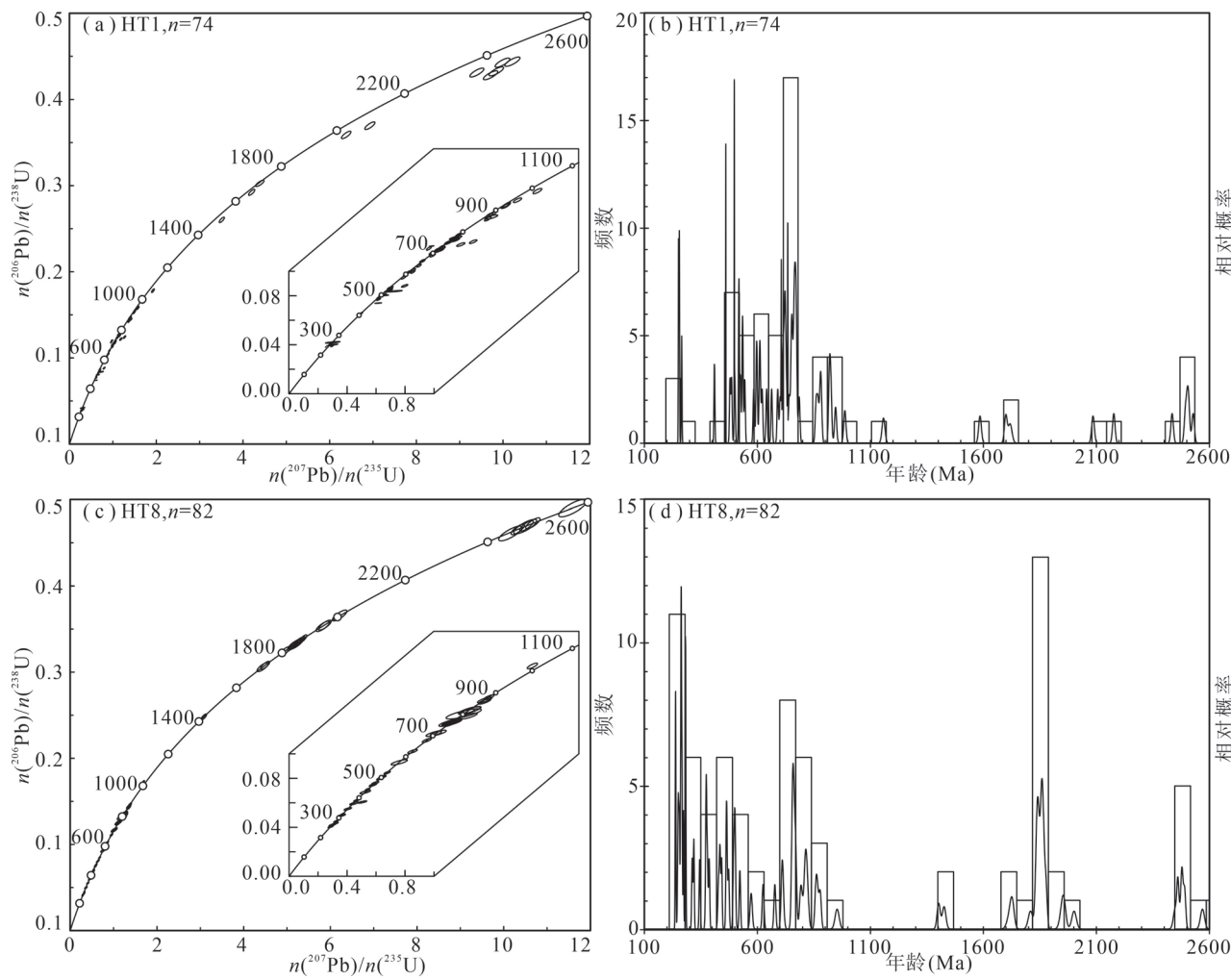


图 7 扬子克拉通西缘下三叠统飞仙关组(HT1)和上三叠统须家河组(HT8)砂岩碎屑锆石 U-Pb 年龄谐和图(a,c)和直方图(b,d)

Fig. 7 Concordia diagrams (a, c) and histogram (b, d) of U-Pb ages for detrital zircons from the sandstones of the Lower Triassic Feixianguan Formation (HT1) and the Upper Triassic Xujiayao Formation (HT8) on the western margin of the Yangtze Craton

#### 4.1 飞仙关组物源区

古水流显示,飞仙关组物源主要来自于西部(图 1),其潜在物源区包括康滇古陆等。

251~265 Ma 锆石年龄与峨眉山大火成岩省侵入岩和酸性岩的时间一致(Hei Huixin et al., 2018)。且铬尖晶石显示,部分物源来自大火成岩省岩石(图 5)。因此,大火成岩省玄武岩及同期岩浆岩为飞仙关组提供物源。且锆石和铬尖晶石呈次棱角状,表明峨眉山玄武岩及同期岩浆岩几乎未经历再旋回过程,为近源沉积。因电气石呈现次圆状,因此该时期沉积物不是电气石的物质来源。460~519 Ma 颗粒碎屑年龄与秦岭造山带的年龄较接近(Wang Xiaoxia et al., 2013; 曾俊杰等, 2021),且锆石颗粒呈次圆状,经历再旋回过程。525~544 Ma 锆

石颗粒呈次圆状、环带清晰,年龄值与康滇古陆的筇竹寺组( $539.4 \pm 2.9$  Ma, Compston et al., 2008)和灯影组凝灰岩( $539.6 \pm 1.4$  Ma, 资金平等, 2017)接近,这些地层应当为母岩。

544~987 Ma 锆石颗粒占比 45.45%, Th/U 比值  $> 0.1$ , 锆石颗粒具有振荡环带,为岩浆成因。部分锆石呈次棱角状,部分呈次圆状,表明近源和长距离搬运的岩石均有。因此,研究区西侧区域上该时期的岩石均可能为飞仙关组提供物源,包括灯影组下部凝灰岩( $553.6 \pm 2.7$  Ma, Yang Chuan et al., 2017)、陡山沱组凝灰岩( $621 \pm 7$  Ma, Zhang Shihong et al., 2005)、闪长岩( $754 \pm 10$  Ma 和  $748 \pm 11$  Ma, Lai Shaocong et al., 2015;  $772.4 \pm 5.5$  Ma, 赖绍聪等, 2017)、苏雄组岩浆岩( $780 \pm 12$  Ma 和  $838 \pm 12$  Ma, 卓

皆文等,2017)和天全花岗岩( $851\pm15$  Ma, 赖绍聪等,2015)等。因表现OIB型特征的碎屑尖晶石以及全部电气石呈次圆状,表明源岩经历了长距离搬运。因电气石部分物源以贫锂花岗岩为主,结合区域飞仙关组的物源特征(张英利等,2016),因此,上述部分源岩经历剥蚀、搬运、沉积等过程,为飞仙关组提供物源。1158~2177 Ma的锆石颗粒较少,且相对分散,没有形成明显的峰值。碎屑锆石颗粒呈次圆状,表明经历长距离的搬运。碎屑锆石古元古代和新太古代年龄主要集中在2435~2494 Ma和2503~2528 Ma,而研究表明扬子西缘古元古代锆石年龄主要为2000~2400 Ma(Wu Yuanbao et al., 2012),2435~2494 Ma和2503~2528 Ma锆石年龄与碧口地块鱼洞子群年龄更接近( $2449\pm4$  Ma, Hui Bo et al., 2017;  $2477\pm18$  Ma, Zhou Guangyan et al., 2018),表明碧口地块的沉积物剥蚀、搬运至扬子西缘。上述源岩中,仅碧口地块发育变沉积岩,因此,电气石的来源为碧口地块。

因此,峨眉山玄武岩和康滇古陆成为飞仙关组重要的物源区,碧口地块等南秦岭造山带少量沉积物经历剥蚀等过程,为飞仙关组的间接物源区。

#### 4.2 须家河组物源区

区域研究成果(Tan Xiucheng et al., 2013; 戴朝成等, 2014; Yan Zhaokun et al., 2019; Yang Wei et al., 2019)和物源方向表明,须家河组物源来自西北,潜在物源区包括康滇古陆、碧口地块等。

228~251 Ma碎屑锆石颗粒10粒,占有效年龄的锆石总数12.50%,锆石Th/U值介于0.36~1.16。锆石呈次棱角状,具有明显的振荡环带(图6),为典型的岩浆成因。与~228 Ma碎屑锆石年龄相当的岩浆作用在康滇古陆很少。南秦岭造山带印支期岩浆作用发育(Qin Jiangfeng et al., 2013; Chen Yanjing et al., 2014),与扬子板块和华北板块的碰撞时间(~244 Ma)一致(Roger et al., 2004)。且碎屑锆石次棱角状表明为近物源。因此,晚三叠世,南秦岭造山带抬升、剥蚀,成为须家河组的物源区。且花岗岩类也是须家河组电气石的主要母岩。

255~387 Ma,峰值年龄为259 Ma,辅助尖晶石的电子探针分析结果表明,峨眉山玄武岩及同期的岩浆岩为须家河组的重要物源区。429~523 Ma锆石年龄较分散,没有明显的峰值,但总体与秦岭造山带的岩浆作用时间一致(Wang Xiaoxia et al., 2013),这表明秦岭造山带岩石隆升、剥蚀、搬运等,成为须家河组的物源区。573~954 Ma锆石颗粒占

比26.25%,Th/U值0.27~2.07(>0.1),锆石颗粒具有振荡环带,为岩浆成因。根据尖晶石电子探针显示,其主要来自岛弧类岩石。区域资料表明,秦岭造山带(包括碧口地块)和康滇古陆均发育新元古代岛弧性质的岩石,且尖晶石呈次圆状,表明经历多次搬运,因此,无法断定尖晶石是来自秦岭造山带还是康滇古陆。康滇古陆中泸定杂岩、泸定安山岩类(Lai Shaocong et al., 2015; 赖绍聪等,2017)、石棉辉长岩(Zhao Junhong et al., 2017)等基性岩浆岩发育尖晶石。同时,北秦岭中商南辉长岩(李惠民等,2006)、天水关子镇岩体(裴先治等,2005)、松树沟辉石岩(董云鹏等,1997; Su Li et al., 2004)等岩浆岩也可发育尖晶石。1720~2004 Ma锆石颗粒较多,且碎屑锆石颗粒呈次圆状,表明经历长距离的搬运。碎屑锆石的峰值年龄1863 Ma与华北板块岩石锆石年龄接近(王洪亮等,2007; 陈岳龙等,2008),如太华杂岩(Xu Xisheng et al., 2009)、花岗岩(Zhao Taiping and Zhou Meifu, 2009)和基性岩墙(胡国辉等,2010)等,表明华北板块的沉积物剥蚀、搬运至扬子西缘。而且扬子西缘古元古代河口群碎屑锆石年龄结果也证明~1800 Ma岩石来自于华北板块(Chen Weiterry et al., 2013)。2453~2494 Ma以及新太古代年龄与碧口地块的峰值年龄2400 Ma(Wu Yuanbao et al., 2012; Hui Bo et al., 2017; Zhou Guangyan et al., 2018)接近,因此,碧口地块岩石是须家河组的母岩。须家河组电气石中变沉积岩可能也来源于古元古代—新太古代岩石。

因此,峨眉山玄武岩、康滇古陆、秦岭造山带(包括碧口地块)和华北板块成为须家河组的物源区。

#### 4.3 三叠纪物源变化及构造响应

电气石探针分析结果显示,三叠纪沉积物源岩主要来自变质板岩、变质砂岩,少量来自贫锂花岗岩类。相比飞仙关组,嘉陵江组和须家河组在贫锂花岗岩类物源区(图4a和图4b中的2区域)比例增加。这表明,更多的花岗岩成为嘉陵江组和须家河组的物源。碎屑锆石分析结果表明,嘉陵江组主要来自康滇古陆新元古代花岗岩,而须家河组则主要来自于秦岭造山带早中生代花岗岩。须家河组在变质板岩和变质砂岩(图4a中4+5区域)比例最多,这表明须家河组时期,更多的变板岩和变砂岩隆升、剥蚀、搬运成为其物源。这可能与碎屑锆石分析的华北板块中较多前寒武纪物质作为沉积物源有关。

尖晶石的探针分析结果表明,飞仙关组以大火

成岩省和洋岛玄武岩类为主,嘉陵江组以洋岛玄武岩类为主,而须家河组以岛弧类为主。研究成果表明,峨眉山玄武岩具有大火成岩省特征(Xu Yigang et al., 2004),飞仙关组和嘉陵江组的洋岛玄武岩类主要来自于新元古代苏雄组,苏雄组玄武岩具有OIB型岩浆特征(Li Xianhua et al., 2002)。须家河组岛弧类岩石在康滇古陆和秦岭造山带分布广泛(Xiao Long et al., 2007; Dong Yunpeng et al., 2011; Zhao Junhong et al., 2017)。结合碎屑锆石分析,早三叠世时期,尖晶石主要来自于峨眉山玄武岩和康滇古陆新元古代岩石,至须家河组时期尖晶石主要来自于康滇古陆和秦岭造山带新元古代岩石。

碎屑锆石表明,三叠纪沉积物的物源主要来自康滇古陆、秦岭造山带和华北板块。来自康滇古陆的沉积物主要是新元古代岩石和峨眉山玄武岩,来自秦岭造山带的沉积物则略有差异:飞仙关组的物源区年龄主要是460~519 Ma和2435~2528 Ma,嘉陵江组无秦岭造山带物源(张英利等,2019),而须家河组物源的年龄值为228~251 Ma、429~523 Ma和2453~2653 Ma(图7d)。来自于华北板块的物源区年龄仅须家河组1720~2004 Ma。

从物源分析看,早三叠世飞仙关组沉积物的主要源区包括峨眉山玄武岩、康滇古陆和南秦岭造山带,嘉陵江组的物源区包括峨眉山玄武岩、康滇古陆和华北地块,而晚三叠世沉积物的主要源区包括峨眉山玄武岩、康滇古陆、秦岭造山带和华北板块。物源的变化主要受沉积时期的构造环境所控制。从早—中三叠世至晚三叠世,构造环境从伸展转换为挤压的前陆盆地,那么沉积物源也发生相应变化。早三叠世飞仙关组至嘉陵江组,构造环境具有继承性,物源区变化不大,随着剥蚀作用的持续,逐渐以新元古代岩石为主要源区。而晚三叠世,区域处于前陆盆地的演化阶段。南秦岭造山带与扬子板块逆时针碰撞,从大巴山、米仓山向西至扬子西缘(Yin An and Nie Shangyou, 1993; Meng Qingren et al., 1999, 2005),碰撞时间逐渐变新,而且扬子西缘北部较早,而南部较晚。受秦岭造山带和扬子板块碰撞影响,须家河组物源区古元古代岩石比例增多,因此研究区北侧秦岭造山带、华北板块抬升,为须家河组提供沉积物源。

## 5 结论

扬子克拉通西缘三叠纪地层出露较好,通过对砂岩重矿物物源的综合分析,得出以下结论:

(1)下三叠统主要源自贫锂花岗岩类及其伴生伟晶岩和细晶岩、变质板岩、变质砂岩、钙质硅酸盐岩和电气石石英岩,上三叠统主要来自贫锂花岗岩类及其伴生伟晶岩和细晶岩、贫钙变质板岩、变质砂岩和电气石石英岩,且自下三叠统至上三叠统变板岩和变砂岩的物源区比重逐渐增加。

(2)下三叠统砂岩主要来自大火成岩省、洋岛玄武岩和岛弧玄武岩类,上三叠统主要来自岛弧玄武岩类。

(3)扬子西缘下三叠统沉积物主要来自峨眉山玄武岩、康滇古陆,少量来自南秦岭造山带,而上三叠统的物源区主要为峨眉山玄武岩、康滇古陆、秦岭造山带和华北板块,主要与不同造山带的隆升有关。

**致谢:**电子探针测试工作得到中国地质大学(北京)电子探针实验室郝金华博士的帮助!碎屑锆石U-Pb测年工作感谢中国地质科学院矿产资源研究所侯可军副研究员的帮助!同时感谢评审专家对本文工作的建议。

## 参 考 文 献 / References

- (The literature whose publishing year followed by a “&” is in Chinese with English abstract; The literature whose publishing year followed by a “#” is in Chinese without English abstract)
- 曹剑, 谭秀成, 陈景山. 2004. 川西南犍为地区下三叠统嘉陵江组沉积相及其演化特征. 高校地质学报, 10(3): 429~439.
- 陈斌, 李勇, 王伟明, 李海兵, 苏德辰, 颜照坤. 2016. 晚三叠世龙门山前陆盆地须家河组物源及构造背景分析. 地质学报, 90(5): 857~872.
- 陈洪德, 张成弓, 黄福喜, 侯明才. 2011. 中上扬子克拉通海西—印支期(泥盆纪—中三叠世)沉积层序充填过程与演化模式. 岩石学报, 27(8): 2281~2298.
- 陈岳龙, 李大鹏, 周建, 张宏飞, 刘飞, 聂兰仕, 蒋丽婷, 柳小明. 2008. 中国西秦岭碎屑锆石U-Pb年龄及其构造意义. 地学前缘, 15(4): 88~107.
- 崔克信. 2004. 中国西南区域古地理及其演化图集. 北京:地震出版社: 1~514.
- 戴朝成, 郑荣才, 任军平, 朱如凯. 2014. 四川前陆盆地上三叠统须家河组物源区分析及其地质意义. 吉林大学学报(地球科学版), 44(4): 1085~1096.
- 董云鹏, 周鼎武, 张国伟. 1997. 东秦岭富水基性杂岩体地球化学特征及其形成环境. 地球化学, 26(3): 79~88.
- 侯可军, 李延河, 田有荣. 2009. LA-MC-ICP-MS锆石微区原位U-Pb定年技术. 矿床地质, 28(4): 481~492.
- 胡国辉, 胡俊良, 陈伟, 赵太平. 2010. 华北克拉通南缘中条山—嵩山地区1.78Ga基性岩墙群的地球化学特征及构造环境. 岩石学报, 26(5): 1563~1576.
- 黄福喜, 陈洪德, 侯明才, 钟怡江, 李洁. 2011. 中上扬子克拉通加里东期(寒武—志留纪)沉积层序充填过程与演化模式. 岩石学报, 27(8): 2299~2317.
- 姜磊, 刘树根, 王自剑, 李智武, 赖东, 何宇, 罗强, 周政, 邓宾. 2019. 上扬子盆地西缘晚白垩世物源变化及指示. 地质论评, 65(2):

- 477~490.
- 赖绍聰,秦江锋,朱韧之,赵少伟. 2015. 扬子地块西缘天全新元古代过铝质花岗岩类成因机制及其构造动力学背景. 岩石学报, 31(8):2245~2258.
- 赖绍聰,朱韧之. 2017. 四川泸定地区新元古代火山岩地球化学特征及其大陆动力学意义. 地球科学与环境学报, 39(4):459~475.
- 李惠民,陈志宏,相振群,李怀坤,陆松年,周红英,宋彪. 2006. 秦岭造山带商南—西峡地区富水杂岩的变辉长岩中斜锆石与锆石U-Pb同位素年龄的差异. 地质通报, 25(6):653~659.
- 林文球,王洪峯,宋华彬. 1982. 四川峨眉龙门洞晚二叠世—早中三叠世地层及其沉积环境. 矿物岩石, 1(3):50~55.
- 刘俊来,唐渊,宋志杰,Dung T M,翟云峰,吴文彬,陈文. 2011. 滇西哀牢山构造带:构造与演化. 吉林大学学报(地球科学版), 41(5):1285~1303.
- 马永生. 2009. 中国南方构造—层序岩相古地理图集. 北京:科学出版社, 102~161.
- 裴先治,李勇,陆松年,陈志宏,丁仁平,胡波,李佐臣,刘会彬. 2005. 西秦岭天水地区关子镇中基性岩浆杂岩体锆石U-Pb年龄及其地质意义. 地质通报, 24(1):23~29.
- 宋谢炎,侯增谦,汪云亮,张成江. 1999. 晚古生代—早中生代扬子板块西缘的构造—岩浆活动. 地质论评, 45(7):868~871.
- 谭富文,潘桂棠,王剑. 2001. 滇西泥盆纪—三叠纪盆—山转换过程与特提斯构造演化. 矿物岩石, 21(3):179~185.
- 田洋,谢国刚,王占令,涂兵,赵小明,曾波夫. 2015. 鄂西南齐岳山须家河组物源及构造背景;来自岩石学、地球化学和锆石年代学的制约. 地球科学, 40(12):2021~2036.
- 王洪亮,何世平,陈隽璐,徐学义,孙勇,第五春荣,李海平. 2007. 北秦岭西段胡店片麻状二长花岗岩LA-ICP-MS锆石U-Pb测年及其地质意义. 中国地质, 34(1):17~25.
- 王正瑛,邓江红. 1982. 四川峨眉龙门洞下三叠统嘉陵江组沉积相. 矿物岩石, 1(3):83~93.
- 王宗起,闫全人,闫臻,王涛,姜春发,高联达,李秋根,陈隽璐,张英利,刘平,谢春林,向忠金. 2009. 秦岭造山带主要大地构造单元的新划分. 地质学报, 83(11):1527~1546.
- 夏磊,闫全人,向忠金,江文,宋博,陈辉明. 2017. 松潘—甘孜地体中部晚三叠世安山质增生弧的确定及其意义. 岩石学报, 33(2):579~604.
- 杨鑫,刘燕红,孙国强,刘兴旺,王保忠,郑建京. 2010. 滇西三江地区中生代盆—山动力学耦合初论. 地质论评, 56(2):196~204.
- 张英利,贾晓彤,王宗起,王坤明,陈木银. 2019. 上扬子西南缘早三叠世嘉陵江组物源分析和构造环境;沉积学、重矿物电子探针和U-Pb年龄的限定. 地质学报, 93(12):3197~3222.
- 张英利,王宗起,王刚,李谦,林健飞. 2016. 上扬子会泽地区早三叠世飞仙关组砂岩物源特征;来自重矿物铬尖晶石和碎屑锆石的限定. 地质论评, 61(1):54~72.
- 郑荣才,李国晖,戴朝成,李楠,王昌勇. 2012. 四川类前陆盆地盆—山耦合系统和沉积学响应. 地质学报, 86(1):170~180.
- 曾俊杰,李康宁,严康,韦乐乐,火兴达,张健鹏. 2021. 西秦岭下三叠统江里沟组构造环境和物源特征. 地质论评, 67(1):69~83.
- 卓皆文,江卓斐,江新胜,王剑,蔡娟娟,熊国庆,陆俊泽,崔晓庄,刘建辉. 2017. 川西新元古代苏雄组层型剖面SHRIMP锆石U-Pb年龄及其地质意义. 地质论评, 63(1):177~188.
- 资金平,贾东,魏国齐,杨振宇,张勇,胡晶,沈淑鑫. 2017. 四川乐山震旦系灯影组火山碎屑岩锆石LA-ICP-MS U-Pb定年及盆地裂陷演化讨论. 地质论评, 63(4):1040~1049.
- Anderson T. 2002. Correction of common lead in U-Pb analyses that do not report  $^{204}\text{Pb}$ . Chemical Geology, 192: 59~79.
- Arai S. 1992. Chemistry of chromian spinel in volcanic rocks as a potential guide to magma chemistry. Mineralogical Magazine, 56: 173~184.
- Armstrong-Altrin J S, Verma S P. 2005. Critical evaluation of six tectonic setting discrimination diagrams using geochemical data of Neogene sediments from known tectonic settings. Sedimentary Geology 177(1~2): 115~129.
- Barnes S J, Roeder P L. 2001. The range of spinel compositions in terrestrial mafic and ultramafic rocks. Journal of Petrology, 42: 2279~2302.
- Brandelik A. 2009. CALCMIN—an EXCEL<sup>TM</sup> visual basic application for calculating mineral structural formulae from electron microprobe analyses. Computers & Geosciences, 35: 1540~1551.
- Cao Jian, Tan Xiucheng, Chen Jingshan. 2004&. Sedimentary facies and their evolution characteristics in Jialingjiang Formation of Qianwei area, southwest Sichuan basin. Geological Journal of China Universities, 10(3): 429~439.
- Chen Bin, Li Yong, Wang Weiming, Li Haibing, Su Dechen, Yan Zhaokun. 2016&. The provenance and tectonic setting of Late Triassic Xujiahe Formation in the Longmenshan foreland basin, SW China. Acta Geologica Sinica, 90(5): 857~872.
- Chen Hongde, Zhang Chenggong, Huang Fuxi, Hou Mingcai. 2011&. Filling process and evolutionary model of sedimentary sequence of Middle—Upper Yangtze craton in Hercynian—Indosinian (Devonian—Middle Triassic). Acta Petrologica Sinica, 27(8): 2281~2298.
- Chen Weiterry, Zhou Meifu, Zhao Xinfu. 2013. Late Paleoproterozoic sedimentary and mafic rocks in the Hekou area, SW China: Implication for the reconstruction of the Yangtze Block in Columbia. Precambrian Research, 231: 61~77.
- Chen Yanjing, Santosh M. 2014. Triassic tectonics and mineral systems in the Qinling Orogen, central China. Geological Journal, 49: 338~358.
- Chen Yuelong, Li Dapeng, Zhou Jian, Zhang Hongfei, Liu Fei, Jiang Lanshi, Jiang Liting, Liu Xiaoming. 2008&. U-Pb ages of zircons in Western Qinling Mountain, China, and their tectonic implications. Earth Science Frontiers, 15(4): 88~107.
- Compston W, Zhang Z C, Cooper J A, Ma G G, Jenkins R J F. 2008. Further SHRIMP geochronology on the Early Cambrian of South China. American Journal of Science, 308: 399~420.
- Cui Kexin. 2004&. Map of regional palaeogeography and its evolution in Southwest China. Beijing: Science Press: 1~514.
- Dai Chaocheng, Zheng Rongcui, Ren Junping, Zhu Rukai. 2014&. Provenance analysis of Xujiahe Formation of Upper Triassic in Sichuan foreland basin and its geological implications. Journal of Jilin University: Earth Science Edition, 44(4): 1085~1096.
- Deng Tao, Li Yong, Wang Zhengjiang, Yu Qian, Dong Shunli, Yan Liang, Hu Wenchao, Chen Bin. 2019. Geochemical characteristics and organic matter enrichment mechanism of black shale in the Upper Triassic Xujiahe Formation in the Sichuan basin: Implications for paleo-weathering, provenance and tectonic setting. Marine and Petroleum Geology, 109: 698~716.
- Dong Yunpeng, Liu Xiaoming, Santosh M, Chen Qing, Zhang Xiaoning, Li Wei, He Dengfeng, Zhang Guowei. 2012. Neoproterozoic accretionary tectonics along the northwestern margin of the Yangtze Block, China: Constraints from zircon U-Pb geochronology and geochemistry. Precambrian Research, 196~197: 247~274.
- Dong Yunpeng, Liu Xiaoming, Santosh M, Zhang Xiaoning, Chen Qing,

- Yang Chen, Yang Zhao. 2011. Neoproterozoic subduction tectonics of the northwestern Yangtze Block in South China: Constrains from zircon U-Pb geochronology and geochemistry of mafic intrusions in the Hannan Massif. *Precambrian Research*, 189(1~2): 66~90.
- Dong Yunpeng, Santosh M. 2016. Tectonic architecture and multiple orogeny of the Qinling Orogenic Belt, Central China. *Gondwana Research*, 29: 1~40.
- Dong Yunpeng, Zhou Dingwu, Zhang Guowei. 1997&. Geochemistry and formation setting of Fushui Complex, eastern Qinling. *Geochimica*, 26(3): 79~88.
- Gehrels G, Johnsson M J, Howell D G. 1999. Detrital zircon geochronology of the Adams Argillite and Nation River Formation, East—Central Alaska, U. S. A. *Journal of Sedimentary Research*, 69: 135~144.
- Hei Huixin, Su Shangguo, Wang Yu, Mo Xuanxue, Luo Zhaozhou, Liu Wengang. 2018. Rhyolites in the Emeishan large igneous province (SW China) with implications for plume-related felsic magmatism. *Journal of Asian Earth Sciences*, 164: 344~365.
- Henry D J, Guidotti C V. 1985. Tourmaline as a petrogenetic indicator mineral: An example from the staurolite-grade metapelites of NW Maine. *American Mineralogist*, 70(1~2): 1~15.
- Henry D J, Novák M, Hawthorne F C, Ertl A, Dutrow B L, Uher P, Pezzotta F. 2011. Nomenclature of the tourmaline-supergroup minerals. *American Mineralogist*, 96: 895~913.
- Hou Kejun, Li Yanhe, Tian Yourong. 2009&. In situ U-Pb zircon dating using laser ablation-multi ion counting-ICP-MS. *Mineral Deposits*, 28(4): 481~492.
- Hu Guohui, Hu Junliang, Chen Wei, Zhao Taiping. 2010&. Geochemistry and tectonic setting of the 1.78 Ga mafic dyke swarms in the Mt. Zhongtiao and Mt. Song areas, the southern margin of the North China Craton. *Acta Petrologica Sinica*, 26(5): 1563~1576.
- Huang Fuxi, Chen Hongde, Hou Mingcai, Zhong Yijiang, Li Jie. 2011&. Filling process and evolutionary model of sedimentary sequence of Middle—Upper Yangtze craton in Caledonian (Cambrian—Silurian). *Acta Petrologica Sinica*, 27(8): 2299~2317.
- Hui Bo, Dong Yunpeng, Cheng Chao, Long Xiaoping, Liu Xiaoming, Yang, Zhao, Sun Shengsi, Zhang Feifei, Varga J. 2017. Zircon U-Pb chronology, Hf isotope analysis and whole-rock geochemistry for the Neoarchean—Paleoproterozoic Yudongzi complex, northwestern margin of the Yangtze craton, China. *Precambrian Research*, 301: 65~85.
- Jiang Lei, Liu Shugen, Wang Zijian, Li Zhiwu, Lai Dong, He Yu, Luo Qiang, Zhou Zheng, Deng Bin. 2019&. Provenance change and its indication of Late Cretaceous in the west margin of Upper Yangtze Basin. *Geological Review*, 65(2): 477~490.
- Kamenetsky V S, Crawford A J, Meffer S. 2001. Factors controlling chemistry of magmatic spinel: An empirical study of associated olivine, Cr-spinel and melt inclusions from primitive rocks. *Journal of Petrology*, 42: 655~671.
- Lai Shaocong, Qin Jiangfeng, Zhu Renzhi, Zhao Shaowei. 2015. Neoproterozoic quartz monzonodiorite association from the Luding—Kangding area: Implications for the interpretation of an active continental margin along the Yangtze Block (South China Block). *Precambrian Research*, 267: 196~208.
- Lai Shaocong, Qin Jiangfeng, Zhu Renzhi, Zhao Shaowei. 2015&. Petrogenesis and tectonic implication of the Neoproterozoic peraluminous granitoids from the Tianquan area, western Yangtze Block, South China. *Acta Petrologica Sinica*, 31(8): 2245~2258.
- Lai Shaocong, Zhu Renzhi. 2017&. Geochemical characteristics and its continental dynamic implication of Neoproterozoic volcanic rocks in Luding area of Sichuan, China. *Journal of Earth Sciences and Environment*, 39(4): 459~475.
- Li Huimin, Chen Zhihong, Xiang Zhenqun, Li Huaikun, Lu Songnian, Zhou Hongying, Song Biao. 2006&. Difference in U-Pb isotope ages between baddeleyite and zircon in metagabbro from the Fushui complex in the Shangnan—Xixia area, Qinling orogen. *Geological Bulletin of China*, 25(6): 653~659.
- Li Xianhua, Li Zhengxiang, Zhou Hanwen, Liu Ying, Kinny P D. 2002. U-Pb zircon geochronology, geochemistry and Nd isotopic study of Neoproterozoic bimodal volcanic rocks in the Kangdian Rift of South China: Implications for the initial rifting of Rodinia. *Precambrian Research*, 113: 135~154.
- Li Yingqiang, Li Shuangjian, He Dengfa, Gao Jian, Wang Yuanchong, Huang Hanyu, Zhang Juntao, Zhang Yong. 2021. Middle Triassic tectono—sedimentary development of Sichuan Basin: Insights into the cratonic differentiation. *Geological Journal*, 56: 1858~1878.
- Lin Wenqiu, Wang Hongfeng, Song Huabin. 1982&. Upper Permian to Lower—Middle Triassic strata and sedimentary environments in Longmendong, Emei, Sichuan. *Journal of Mineralogy and Petrology*, 1(3): 50~55.
- Liu Junlai, Tang Yuan, Song Zhiping, Dung T M, Zhai Yunfeng, Wu Wenbin, Chen Wen. 2011&. The Ailaoshan belt in western Yunnan: Tectonic framework and tectonic evolution. *Journal of Jilin University (Earth Science Edition)*, 41(5): 1285~1303.
- Liu Yongsheng, Gao Shan, Hu Zhaochu, Gao Changgui, Zong Keqing, Wang Dongbing. 2010. Continental and oceanic crust recycling-induced melt—peridotite interactions in the Trans-North China Orogen: U-Pb dating, Hf isotopes and trace elements in zircons from mantle xenoliths. *Journal of Petrology*, 51: 537~571.
- Ludwig K R. 2003. User's manual for Isoplot 3.0: Geochronological toolkit for Microsoft Excel. Berkeley Geochronology Center Special Publication, 4: 1~70.
- Ma Yongsheng. 2009&. Sequence Stratigraphy and Palaeogeography of South China. Beijing: Science Press: 102~161.
- Meng Qingren, Wang Erqi, Hu Jianmin. 2005. Mesozoic sedimentary evolution of northwest Sichuan Basin: Implications for continued clockwise rotation of the South China Block. *Geological Society of America Bulletin*, 117: 396~410.
- Meng Qingren, Zhang Guowei. 1999. Timing of collision of North and South China blocks: Controversy and reconciliation. *Geology*, 27: 123~126.
- Moecher D P, Samson S D. 2006. Differential zircon fertility of source terranes and natural bias in the detrital zircon record: Implications for sedimentary provenance analysis. *Earth and Planetary Science Letters*, 247: 252~266.
- Mu Hongxu, Yan Danping, Qiu Liang, Yang Wenxin, Kong Ruoyan, Gong Lingxiao, Li Shubing. 2019. Formation of the Late Triassic western Sichuan foreland basin of the Qinling Orogenic Belt, SW China: Sedimentary and geochronological constraints from the Xujiahe Formation. *Journal of Asian Earth Sciences*, 183: 103938.
- Pei Xianzhi, Li Yong, Lu Songnian, Chen Zhihong, Ding Saping, Hu Bo, Li Zuochen, Liu Huibin. 2005&. Zircon U-Pb ages of the Guanzizhen intermediate—basic igneous complex in Tianshui area, West Qinling, and their geological significance. *Geological Bulletin of China*, 24(1): 23~29.

- Qin Jiangfeng, Lai Shaocong, Li Yonfei. 2013. Multistage granitic magmatism during exhumation of subducted continental lithosphere: Evidence from the Wulong pluton, South Qinling. *Gondwana Research*, 24: 1108~1126.
- Roger F, Malavieille J, Leloup P H, Calassou S, Xu Z. 2004. Timing of granite emplacement and cooling in the Songpan—Garzê Fold Belt (eastern Tibetan Plateau) with tectonic implications. *Journal of Asian Earth Sciences*, 22: 465~481.
- Sircombe K N. 1999. Tracing provenance through the isotope ages of littoral and sedimentary detrital zircon, eastern Australia. *Sedimentary Geology*, 124: 47~67.
- Song Xieyan, Hou zengqian, Wang Yunliang, Zhang Chengjiang. 1999&. The Late Paleozoic—Early Mesozoic tectono-magmatism in the western margin of the Yangtze Plate. *Geological Review*, 45 (7): 868~871.
- Su Li, Song Shuguang, Song Biao, Zhou Dingwu, Hao Jianrong. 2004. SHRIMP zircon U-Pb ages of garnet pyroxenite and Fushui gabbroic complex in Songshugou region and constraints on tectonic evolution of Qinling Orogenic Belt. *Chinese Science Bulletin*, 49: 1307~1310.
- Tan Fuwen, Pan Guitang, Wang Jian. 2001&. Devonian—Triassic basin-range transformation and the tectonic evolution of Paleo-Tethys in western Yunnan, China. *Journal of Mineralogy and Petrology*, 21 (3): 179~185.
- Tan Xiucheng, Xia Qingsong, Chen Jingshan, Li Ling, Liu Hong, Luo Bing, Xia Jiwen, Yang Jiajing. 2013. Basin-scale sand deposition in the Upper Triassic Xujiahe Formation of the Sichuan Basin, Southwest China: Sedimentary framework and conceptual model. *Journal of Earth Science*, 24: 89~103.
- Tian Yang, Xie Guogang, Wang Zhanling, Tu Bing, Zhao Xiaoming, Zeng Bofu. 2015&. Provenance and tectonic settings of Triassic Xujiahe Formation in Qiyueshan area, southwest Hubei: Evidence from petrology, geochemistry and zircon U-Pb ages of clastic rocks. *Earth Science*, 40(12): 2021~2036.
- von Eynatten H, Dunkl I. 2012. Assessing the sediment factory: The role of single grain analysis. *Earth Science Reviews*, 115: 97~120.
- Wang Hongliang, He Shiping, Chen Junlu, Xu Xueyi, Sun Yong, Diwu Chunrong, Li Haiping. 2007&. LA-ICPMS zircon U-Pb dating of the Hidian gneissic monzogranite the western segment of the North Qinling and its geological significance. *Geology in China*, 134 (1): 17~25.
- Wang Wei, Liu Shuwen, Feng Yonggang, Li Qiugen, Wu Fenghui, Wang Zongqi. 2012. Chronology, petrogenesis and tectonic setting of the Neoproterozoic Tongchang dioritic pluton at the northwestern margin of the Yangtze block: Constraints from geochemistry and zircon U—Pb—Hf isotopic systematic. *Gondwana Research*, 22: 699~716.
- Wang Xiaoxia, Wang Tao, Zhang Chengli. 2013. Neoproterozoic, Paleozoic, and Mesozoic granitoid magmatism in the Qinling Orogen, China: Constraints on orogenic process. *Journal of Asian Earth Sciences*, 72: 129~151.
- Wang Zhengying, Deng Jianghong. 1982&. Tidal flat deposit of Lower Triassic Jialingjiang Formation in EmeiLongmendong, Sichuan. *Journal of Mineralogy and Petrology*, 1(3): 83~93.
- Wang Zongqi, Yan Quanren, Yan Zhen, Wang Tao, Jiang Chunfa, Gao Lianda, Li Qiugen, Chen Junlu, Zhang Yingli, Liu Ping, Xie Chunlin, Xiang Zhongjin. 2009&. New division of the main tectonic units of the Qinling orogenic belt, Central China. *Acta Geologica Sinica*, 83(11): 1527~1546.
- Wu Yuanbao, Gao Shan, Zhang Hongfei, Zheng Jianping, Liu Xiaochi, Wang Hao, Gong Hujun, Zhou Lian, Yuan Honglin. 2012. Geochemistry and zircon U-Pb geochronology of Paleoproterozoic arc related granitoid in the Northwestern Yangtze Block and its geological implications. *Precambrian Research*, 200~203: 26~37.
- Xia Lei, Yan Quanren, Xiang Zhongjin, Jiang Wen, Song Bo, Chen Huiming. 2017&. Late Triassic andesitic accretionary arc in the central Songpan—Ganzi terrane and its tectonic significance. *Acta Petrologica Sinica*, 33(2): 579~604.
- Xiao Long, Zhang Hongfei, Ni Pingze, Xiang Hua, Liu Xiaoming. 2007. LAICP-MS U-Pb zircon geochronology of early Neoproterozoic mafic—intermediate intrusions from NW margin of the Yangtze Block, South China: Implications for tectonic evolution. *Precambrian Research*, 154: 221~235.
- Xu Chunming, Gehenn J M, Zhao Dahua, Xie Geyun, Teng Meekee. 2015. The fluvial and lacustrine sedimentary systems and stratigraphic correlation in the Upper Triassic Xujiahe Formation in Sichuan Basin, China. *AAPG Bulletin*, 99: 2023~2041.
- Xu Xisheng, William L, Griffin X M, O'Reilly S Y, He Zhenyu, Zhang Chengli. 2009. The Taihua Group on the southern margin of the North China craton: Further insights from U-Pb ages and Hf isotope compositions of zircons. *Mineralogy and Petrology*, 97: 43~59.
- Xu Yigang, He Bin, Chung S-L, Menzies M A, Frey F A. 2004. Geologic, geochemical, and geophysical consequences of plume involvement in the Emeishan flood-basalt province. *Geology*, 32: 917~920.
- Yan Danping, Zhou Meifu, Song Honglin, Wang Xinwen, Malpas J. 2003. Origin and tectonic significance of a Mesozoic multi-layer overthrust system within the Yangtze Block (South China). *Tectonophysics*, 361: 239~254.
- Yan Zhaokun, Tian Yuntiao, Li Rui, Vermeesch P, Sun Xilin, Li Yong, Rittner M, Carter A, Shao Congjian, Huang Hu, Ji Xiangtian. 2019. Late Triassic tectonic inversion in the upper Yangtze Block: Insights from detrital zircon U-Pb geochronology from southwestern Sichuan Basin. *Basin Research*, 31: 92~113.
- Yang Chuan, Li Xianhua, Zhu Maoyan, Condon D J. 2017. SIMS U-Pb zircon geochronological constraints on upper Ediacaran stratigraphic correlations, South China. *Geological Magazine*, 154: 1202~1216.
- Yang Wei, Zuo Rusi, Chen Dongxia, Jiang Zhenxue, Guo Lishuang, Liu Ziyi, Chen Rong, Zhang Yunpeng, Zhang Ziya, Song Yan, Luo Qun, Wang Qianyou, Wang Jianbao, Chen Lei, Li Yaohua, Zhang Chen. 2019. Climate and tectonic-driven deposition of sandwiched continental shale units: New insights from petrology, geochemistry, and integrated provenance analysis (the western Sichuan subsiding Basin, Southwest China). *International Journal of Coal Geology*, 211: 103227.
- Yang Xin, Liu Yanhong, Sun Guoqiang, Liu Xingwang, Wang Baozhong, Zheng Jianjing. 2010&. Initial exploration to Mesozoic basin—orogen dynamical coupling of “Sanjiang” (Nujiang River—Jinsha River—Lancang River) region, western Yunnan. *Geological Review*, 56(2): 196~204.
- Yin An, Nie Shangyou. 1993. An indentation model for the North and South China collision and the development of the Tan-Lu and Honam Fault systems, Eastern Asia. *Tectonics*, 12(4): 801~813.
- Zeng Junjie, Li Kangning, Yan Kang, Wei Lele, Huo Xingda, Zhang Jianpeng. 2021&. Tectonic setting and provenance characteristics of the Lower Triassic Jiangligou Formation in West Qinling—

- Constraints from geochemistry of clastic rocks and U-Pb geochronology of detrital zircon. *Geological Review*, 67(1): 69~83.
- Zhang Shihong, Jiang Ganqing, Zhang Junming, Song Biao, Kennedy M J, Christie-Blick N. 2005. U-Pb sensitive high-resolution ion microprobe ages from the Doushantuo Formation in South China: Constraints on late Neoproterozoic glaciations. *Geology*, 33: 473~476.
- Zhang Yingli, Jia Xiaotong, Wang Zongqi. 2019. Provenance of the Late Permian Xuanwei Formation in the Upper Yangtze Block: Constraints from the sedimentary record and tectonic implications. *Acta Geologica Sinica (English Edition)*, 93(6), 1673~1686.
- Zhang Yong, Jia Dong, Shen Li, Yin Hongwei, Chen Zhuxin, Li Haibin, Li Zhigang, Sun Chuang. 2015. Provenance of detrital zircons in the Late Triassic Sichuan foreland basin: Constraints on the evolution of the Qinling Orogen and Longmen Shan thrust-fold belt in central China. *International Geology Review*, 57: 1806~1824.
- Zhang Yingli, Jia Xiaotong, Wang Zongqi, Wang Kunming, Chen Mu Yin. 2019&. Provenance analysis and tectonic setting of Early Triassic Jialingjiang Formation in the southwestern Upper Yangtze area: Evidence from sedimentology, heavy mineral electron probe microanalysis and U-Pb dating. *Acta Geologica Sinica*, 93(12): 3197~3222.
- Zhang Yingli, Wang Zongqi, Wang Gang, Li Qian, Lin Jianfei. 2016&. Chemical spinel, zircon age constraints on the provenance of Early Triassic Feixianguan Formation sandstones from Huize area, Upper Yangtze region. *Geological Review*, 61(1): 54~72.
- Zhao Junhong, Asimow P D, Zhou Meifu, Zhang Jian, Yan Danping, Zheng Jianping. 2017. An Andean-type arc system in Rodinia constrained by the Neoproterozoic Shimian ophiolite in South China. *Precambrian Research*, 296: 93~111.
- Zhao Taiping, Zhou Meifu. 2009. Geochemical constraints on the tectonic setting of Paleoproterozoic A-type granites in the southern margin of the North China Craton. *Journal of Asian Earth Sciences*, 36: 183~195.
- Zheng Rongcui, Li Guohui, Dai Chaocheng, Li Nan, Wang Changyong. 2012&. Basin—mountain coupling system and its sedimentary response in Sichuan analogous foreland basin. *Acta Geologica Sinica*, 86(1): 170~180.
- Zhou Guangyan, Wu Yuanbao, Li Long, Zhang Wenxiang, Zheng Jianping, Wang Hao, Yang Saihong. 2018. Identification of ca. 2.65 Ga TTGs in the Yudongzi complex and its implications for the early evolution of the Yangtze Block. *Precambrian Research*, 314: 240~263.
- Zhu Min, Chen Hanling, Zhou Jing, Yang Shufeng. 2017. Provenance change from the Middle to Late Triassic of the southwestern Sichuan basin, Southwest China: Constraints from the sedimentary record and its tectonic significance. *Tectonophysics*, 700~701: 92~107.
- Zhuo Jiwen, Jiang Zhuofei, Jiang Xinsheng, Wang Jian, Cai Juanjuan, Xiong Guoqing, Lu Junze, Cui Xiaozhuang, Liu Jianhui. 2017&. SHRIMP zircon U-Pb ages for the stratotype section of Neoproterozoic Suxiong Formation in western Sichuan province and their geological significance. *Geological Review*, 63(1): 177~188.
- Zi Jinping, Jia Dong, Wei Guoqi, Yang Zhenyu, Zhang Yong, Hu Jing, Shen Shuxin. 2017&. LA-ICP-MS U-Pb zircon ages of volcaniclastic beds of the third member of the Sinian (Ediacaran) Dengying Formation in Leshan, Sichuan, and a discussion on the rift evolution in the Basin. *Geological Review*, 63(4): 1040~1049.

## Provenance analysis of Triassic sediments in the Yingjing area on the western margin of the Yangtze Craton

ZHANG Yingli<sup>1)</sup>, JIA Xiaotong<sup>2)</sup>, WANG Kunming<sup>1)</sup>, WANG Zongqi<sup>1)</sup>, CHEN Mu Yin<sup>3)</sup>

- 1) MNR Key Laboratory of Metallogeny and Mineral Assessment, Institute of Mineral Resources, Chinese Academy of Geological Sciences, Beijing, 100037;
- 2) Information Center of Zhejiang Earthquake Agency, Hangzhou, 310013;
- 3) Changqing Division, China Petroleum Logging Co. LTD. Xi'an, 710201

**Objectives:** The western margin of the Yangtze Craton was an extensional setting in the Early Triassic and a foreland basin in the Late Triassic. The well-preserved Triassic sediments on the western margin of the Yangtze Craton are ideal targets for studying the sedimentary provenance response to tectonic transformation.

**Methods:** Based on the geological work, the heavy mineral electron probe microanalysis and detrital zircon U-Pb dating were carried out on the Triassic sandstones in this paper.

**Results:** The results of tourmaline electron probe microanalysis show that the Lower Triassic sediments are mainly derived from the granitoids and their associated pegmatites and aplites, metapelites and metapsammites, calc-silicate rocks, and quartz-tourmaline rocks, while the Upper Triassic sediments are mainly derived from the granitoids and their associated pegmatites and aplites, Ca-poor metapelites and metapsammites, and quartz-tourmaline rocks. The proportion of metapelites and metapsammites gradually increases from Lower Triassic to Upper Triassic. Spinel results show that the Lower Triassic sandstones are mainly from large igneous provinces, oceanic island basalts and island arc basalts, while the Upper Triassic sediments are mainly derived from island arc basalts. Detrital zircon U-Pb dating results show that the Early Triassic detrital zircon peaks are 251~265 Ma, 460~535 Ma, and 544~987 Ma while the Late Triassic detrital zircon peaks are 228~251 Ma, 255~387 Ma, 429~523 Ma, 573~954 Ma, 1720~2004 Ma and 2453~2494

Ma.

**Conclusions:** Comprehensive analysis show that the sediments of the Lower Triassic were mainly from Emeishan basalt, Kangdian Oldland and secondary from South Qinling orogenic belt. However, source areas of the Upper Triassic are mainly Emeishan basalt, Kangdian Oldland, Qinling orogenic belt, and North China plate. The differences of provenance in Triassic are mainly related to the collision between the Qinling orogenic belt and the Yangtze plate in the Late Triassic.

**Keywords:** Provenance analysis; heavy mineral assemblage; detrital zircon geochronology; Triassic; western margin of the Yangtze Craton

**Acknowledgements:** This research was financially supported by the Deep Resources Exploration and Mining Project (Grant No. 2019YFC0605202), National Natural Science Foundation of China (No. 41302080), and Chinese Geological Survey (No. DD20201173).

**First author:** ZHANG Yingli, male, born in 1979, doctor, professor of senior engineer, mainly engaged in basin tectonic and sedimentology; Email: yinglizh@126.com

**Manuscript received on:** 2020-12-07; **Accepted on:** 2021-04-12; **Network published on:** 2021-04-20

**Doi:** 10.16509/j.georeview.2021.04.123

**Edited by:** ZHAO Xue, ZHANG Yuxu

附表 1 扬子克拉通西缘下三叠统飞仙关组(HT1)和上三叠统须家河组(HT8)砂岩电气石电子探针数据表

Annexed Table 1 Representative chemical composition of the detrital tourmalines from the Lower Triassic Feixianguan Formation ( HT1 ) and the Upper Triassic Xujiahe Formation ( HT8 ) sandstones on the western margin of the Yangtze Craton

样品号	主量元素(%)												原子数(个)													
	SiO <sub>2</sub>	TiO <sub>2</sub>	Al <sub>2</sub> O <sub>3</sub>	Cr <sub>2</sub> O <sub>3</sub>	FeO	MgO	CaO	MnO	Na <sub>2</sub> O	K <sub>2</sub> O	H <sub>2</sub> O*	B <sub>2</sub> O <sub>3</sub> *	Li <sub>2</sub> O*	Total	Si	Ti	Cr	Al	Fe <sup>2+</sup>	Mg	Mn	Li*	Ca	Na	K	γ
飞仙关组样品(HT1)																										
HT1-1	34.06	0.92	26.83	0.07	14.73	4.72	0.39	0.06	2.87	0.07	3.42	9.91	0.00	98.05	5.97	0.12	0.01	5.55	2.16	1.24	0.01	0.00	0.07	0.97	0.02	0.00
HT1-2	34.32	0.42	34.34	0.02	9.20	3.98	0.37	0.08	1.63	0.05	3.57	10.36	0.14	98.49	5.76	0.05	0.00	6.79	1.29	1.00	0.01	0.09	0.07	0.53	0.01	0.39
HT1-3	33.21	0.52	31.69	0.00	13.23	1.92	1.15	0.12	1.78	0.06	3.45	9.99	0.32	97.44	5.78	0.07	0.00	6.50	1.92	0.50	0.02	0.22	0.21	0.60	0.01	0.17
HT1-4	34.82	1.65	30.12	0.04	9.19	5.28	0.09	0.06	2.69	0.02	3.53	10.24	0.29	98.01	5.91	0.21	0.01	6.03	1.30	1.34	0.01	0.20	0.02	0.89	0.00	0.09
HT1-5	35.31	0.40	27.73	0.02	9.99	8.10	0.87	0.05	2.55	0.08	3.53	10.23	0.00	98.85	6.00	0.05	0.00	5.55	1.42	2.05	0.01	0.00	0.16	0.84	0.02	0.00
HT1-6	36.25	0.15	31.55	0.12	4.27	9.29	0.23	0.00	3.05	0.01	3.66	10.61	0.12	99.29	5.94	0.02	0.02	6.09	0.59	2.27	0.00	0.08	0.04	0.97	0.00	0.00
HT1-7	33.06	0.87	28.65	0.00	8.68	7.76	2.17	0.03	1.96	0.06	3.46	10.02	0.04	96.74	5.73	0.11	0.00	5.86	1.26	2.01	0.00	0.03	0.40	0.66	0.01	0.00
HT1-8	34.28	1.23	31.85	0.03	9.60	4.94	0.62	0.00	2.10	0.06	3.56	10.30	0.19	98.75	5.78	0.16	0.00	6.33	1.35	1.24	0.00	0.13	0.11	0.69	0.01	0.19
HT1-9	34.76	0.64	27.37	0.14	7.04	10.50	2.86	0.05	1.45	0.07	3.55	10.29	0.00	98.72	5.87	0.08	0.02	5.45	0.99	2.64	0.01	0.00	0.52	0.47	0.01	0.00
HT1-10	34.57	0.87	30.17	0.06	8.61	7.44	0.81	0.00	2.40	0.06	3.56	10.31	0.00	98.84	5.83	0.11	0.01	5.99	1.21	1.87	0.00	0.00	0.15	0.78	0.01	0.06
HT1-11	35.14	1.69	29.69	0.03	8.35	6.95	0.93	0.07	2.13	0.05	3.58	10.37	0.17	99.14	5.89	0.21	0.00	5.86	1.17	1.74	0.01	0.11	0.17	0.69	0.01	0.13
HT1-12	34.78	0.42	33.46	0.07	5.46	8.14	1.70	0.02	0.49	0.29	3.64	10.54	0.00	99.02	5.73	0.05	0.01	6.50	0.75	2.00	0.00	0.00	0.30	0.16	0.06	0.48
HT1-13	35.88	1.61	29.03	0.00	5.56	9.48	1.17	0.05	2.44	0.04	3.63	10.52	0.16	99.57	5.93	0.20	0.00	5.65	0.77	2.34	0.01	0.11	0.21	0.78	0.01	0.01
HT1-14	34.44	1.24	28.31	0.05	9.85	6.12	0.52	0.08	2.65	0.14	3.47	10.06	0.15	97.08	5.95	0.16	0.01	5.76	1.42	1.58	0.01	0.11	0.10	0.89	0.03	0.00
HT1-15	34.22	0.88	33.01	0.37	5.61	7.26	0.65	0.04	2.13	0.03	3.60	10.43	0.11	98.32	5.70	0.11	0.05	6.48	0.78	1.80	0.01	0.07	0.12	0.69	0.01	0.19
HT1-16	34.82	0.42	34.30	0.04	10.17	2.73	0.19	0.04	1.78	0.08	3.58	10.37	0.32	98.84	5.84	0.05	0.01	6.77	1.43	0.68	0.01	0.22	0.03	0.58	0.02	0.37
HT1-17	32.72	0.59	32.52	0.06	7.58	6.59	1.11	0.00	2.02	0.06	3.51	10.16	0.00	96.94	5.60	0.08	0.01	6.55	1.08	1.68	0.00	0.00	0.20	0.67	0.01	0.11
HT1-18	35.47	0.56	32.30	0.08	7.61	6.21	0.50	0.06	2.49	0.08	3.63	10.51	0.25	99.74	5.87	0.07	0.01	6.30	1.05	1.53	0.01	0.17	0.09	0.80	0.02	0.10
HT1-19	35.12	0.40	31.54	0.04	6.36	7.37	0.23	0.04	2.59	0.02	3.57	10.35	0.10	97.75	5.89	0.05	0.01	6.24	0.89	1.84	0.01	0.07	0.04	0.84	0.00	0.11
HT1-20	35.41	0.66	29.86	0.00	7.90	7.76	1.55	0.12	1.82	0.04	3.59	10.39	0.08	99.19	5.92	0.08	0.00	5.89	1.11	1.93	0.02	0.05	0.28	0.59	0.01	0.12
HT1-21	35.46	0.38	28.83	0.05	7.33	8.91	0.82	0.05	2.71	0.06	3.56	10.32	0.00	98.49	5.97	0.05	0.01	5.72	1.03	2.24	0.01	0.00	0.15	0.88	0.01	0.00
HT1-22	33.81	0.88	33.23	0.06	8.09	4.73	0.44	0.06	1.78	0.05	3.53	10.23	0.19	97.07	5.74	0.11	0.01	6.65	1.15	1.20	0.01	0.13	0.08	0.59	0.01	0.32
HT1-23	34.35	0.85	29.28	0.06	8.65	7.45	1.75	0.03	2.04	0.04	3.53	10.23	0.10	98.36	5.83	0.11	0.01	5.86	1.23	1.89	0.00	0.07	0.32	0.67	0.01	0.00
HT1-24	35.26	0.64	33.32	0.00	7.64	5.63	0.39	0.02	2.05	0.04	3.62	10.50	0.20	99.31	5.84	0.08	0.00	6.50	1.06	1.39	0.00	0.14	0.07	0.66	0.01	0.27
HT1-25	35.07	0.63	31.90	0.00	6.96	7.04	0.47	0.01	2.53	0.05	3.60	10.43	0.15	98.84	5.84	0.08	0.00	6.26	0.97	1.75	0.00	0.10	0.08	0.82	0.01	0.09
HT1-26	35.49	0.83	30.34	0.01	6.62	8.09	0.60	0.00	2.69	0.01	3.60	10.43	0.13	98.84	5.92	0.10	0.00	5.96	0.92	2.01	0.00	0.09	0.11	0.87	0.00	0.02
HT1-27	35.21	1.55	30.02	0.01	8.63	7.28	2.10	0.00	1.70	0.02	3.63	10.52	0.24	100.90	5.82	0.19	0.00	5.84	1.19	1.79	0.00	0.16	0.37	0.54	0.00	0.08
HT1-28	35.58	1.53	29.85	0.05	7.93	7.46	0.35	0.05	2.60	0.06	3.60	10.44	0.09	99.60	5.92	0.19	0.01	5.86	1.10	1.85	0.01	0.06	0.06	0.84	0.01	0.09
HT1-29	35.87	1.73	25.25	0.00	10.12	9.12	1.15	0.00	2.50	0.03	3.54	10.27	0.01	99.59	6.07	0.22	0.00	5.04	1.43	2.30	0.00	0.01	0.21	0.82	0.01	0.00
HT1-30	36.36	0.44	34.53	0.04	4.87	7.28	0.55	0.01	2.22	0.04	3.74	10.84	0.29	101.19	5.83	0.05	0.00	6.53	0.65	1.74	0.00	0.19	0.09	0.69	0.01	0.21

样品号	主量元素(%)													原子数(个)												
	SiO <sub>2</sub>	TiO <sub>2</sub>	Al <sub>2</sub> O <sub>3</sub>	Cr <sub>2</sub> O <sub>3</sub>	FeO	MgO	CaO	MnO	Na <sub>2</sub> O	K <sub>2</sub> O	H <sub>2</sub> O <sup>*</sup>	B <sub>2</sub> O <sub>3</sub> <sup>*</sup>	Li <sub>2</sub> O <sup>*</sup>	Total	Si	Ti	Cr	Al	Fe <sup>2+</sup>	Mg	Mn	Li <sup>*</sup>	Ca	Na	K	γ
HT1-31	35.25	0.65	33.85	0.04	5.93	6.55	0.35	0.00	2.38	0.06	3.66	10.59	0.26	99.56	5.78	0.08	0.01	6.55	0.81	1.60	0.00	0.17	0.06	0.76	0.01	0.17
HT1-32	34.55	0.49	34.28	0.00	13.15	0.96	0.23	0.16	1.75	0.03	3.56	10.33	0.31	99.80	5.81	0.06	0.00	6.80	1.85	0.24	0.02	0.21	0.04	0.57	0.01	0.38
HT1-33	34.69	0.55	29.49	0.09	10.06	6.53	0.33	0.00	2.83	0.02	3.52	10.19	0.00	98.30	5.91	0.07	0.01	5.93	1.43	1.66	0.00	0.00	0.06	0.94	0.00	0.00
HT1-34	35.46	1.06	31.50	0.03	7.49	6.95	0.97	0.02	1.75	0.05	3.62	10.49	0.13	99.53	5.87	0.13	0.00	6.15	1.04	1.72	0.00	0.08	0.17	0.56	0.01	0.25
HT1-35	35.50	1.76	27.76	0.02	8.62	7.49	1.31	0.03	2.34	0.09	3.56	10.31	0.27	99.05	5.98	0.22	0.00	5.51	1.22	1.88	0.00	0.18	0.24	0.76	0.02	0.00
HT1-36	37.56	0.25	31.18	0.00	4.32	9.49	0.16	0.02	2.97	0.05	3.72	10.79	0.28	100.79	6.05	0.03	0.00	5.92	0.58	2.28	0.00	0.18	0.03	0.93	0.01	0.03
HT1-37	34.88	0.77	32.82	0.01	7.75	5.17	0.22	0.00	2.26	0.09	3.58	10.37	0.29	98.19	5.84	0.10	0.00	6.48	1.09	1.29	0.00	0.20	0.04	0.73	0.02	0.21
HT1-38	34.22	0.40	35.32	0.01	8.23	4.27	0.49	0.02	1.54	0.05	3.60	10.44	0.17	98.74	5.70	0.05	0.00	6.93	1.15	1.06	0.00	0.11	0.09	0.50	0.01	0.40
HT1-39	34.53	0.85	32.56	0.00	8.61	4.76	0.38	0.00	2.19	0.04	3.56	10.31	0.28	98.06	5.82	0.11	0.00	6.47	1.21	1.20	0.00	0.19	0.07	0.72	0.01	0.21

须家河组样品(HT8)

HT8-1	34.75	0.19	34.09	0.02	12.77	2.18	0.33	0.14	2.10	0.06	3.60	10.43	0.21	100.87	5.79	0.02	0.00	6.70	1.78	0.54	0.02	0.14	0.06	0.68	0.01	0.25
HT8-2	36.66	0.54	31.01	0.00	9.13	6.61	0.36	0.00	2.66	0.01	3.66	10.62	0.14	101.40	6.00	0.07	0.00	5.98	1.25	1.61	0.00	0.09	0.06	0.84	0.00	0.09
HT8-3	36.38	0.97	30.47	0.10	9.07	6.73	0.61	0.03	2.69	0.00	3.66	10.61	0.20	101.51	5.96	0.12	0.01	5.88	1.24	1.64	0.00	0.13	0.11	0.85	0.00	0.04
HT8-4	35.73	1.21	33.75	0.10	9.56	4.39	0.63	0.12	2.29	0.01	3.71	10.74	0.38	102.62	5.78	0.15	0.01	6.44	1.29	1.06	0.02	0.25	0.11	0.72	0.00	0.17
HT8-5	35.10	1.27	32.54	0.06	8.92	5.16	1.24	0.15	1.85	0.13	3.64	10.56	0.36	100.99	5.77	0.16	0.01	6.31	1.23	1.27	0.02	0.24	0.22	0.59	0.03	0.16
HT8-6	35.46	0.78	33.84	0.01	9.61	3.90	0.53	0.18	2.36	0.04	3.66	10.62	0.42	101.41	5.81	0.10	0.00	6.53	1.32	0.95	0.02	0.28	0.09	0.75	0.01	0.15
HT8-7	35.37	0.46	32.59	0.00	14.98	1.26	0.11	0.12	2.42	0.00	3.59	10.40	0.27	101.57	5.91	0.06	0.00	6.42	2.09	0.31	0.02	0.18	0.02	0.78	0.00	0.20
HT8-8	34.71	0.48	34.02	0.00	13.38	1.93	0.72	0.07	1.92	0.06	3.61	10.47	0.27	101.65	5.76	0.06	0.00	6.65	1.86	0.48	0.01	0.18	0.13	0.62	0.01	0.24
HT8-9	36.38	1.04	34.15	0.05	8.06	5.15	0.53	0.15	2.18	0.02	3.74	10.84	0.38	102.67	5.83	0.13	0.01	6.46	1.08	1.23	0.02	0.25	0.09	0.68	0.00	0.23
HT8-10	36.49	1.14	31.16	0.10	8.00	6.91	0.78	0.03	2.55	0.06	3.69	10.70	0.30	101.91	5.93	0.14	0.01	5.96	1.09	1.67	0.00	0.19	0.14	0.80	0.01	0.05
HT8-11	36.59	1.49	31.02	0.47	5.01	8.68	0.99	0.00	2.75	0.08	3.73	10.82	0.40	102.04	5.88	0.18	0.06	5.87	0.67	2.08	0.00	0.26	0.17	0.86	0.02	0.00
HT8-12	37.36	0.79	33.47	0.10	6.23	6.63	0.49	0.00	2.42	0.09	3.77	10.93	0.44	102.73	5.94	0.09	0.01	6.27	0.83	1.57	0.00	0.28	0.08	0.75	0.02	0.15
HT8-13	36.10	2.11	30.72	0.24	6.05	7.87	1.80	0.00	2.12	0.08	3.72	10.77	0.52	102.10	5.83	0.26	0.03	5.84	0.82	1.89	0.00	0.34	0.31	0.66	0.02	0.01
HT8-14	37.07	0.94	33.26	0.14	4.59	7.84	1.49	0.00	1.93	0.07	3.78	10.96	0.50	102.58	5.88	0.11	0.02	6.21	0.61	1.85	0.00	0.32	0.25	0.59	0.01	0.14
HT8-15	35.66	0.57	33.39	0.32	9.87	3.88	0.30	0.00	2.12	0.03	3.64	10.55	0.32	100.64	5.88	0.07	0.04	6.49	1.36	0.95	0.00	0.21	0.05	0.68	0.01	0.26
HT8-16	36.36	0.94	33.26	0.15	7.67	5.81	1.13	0.20	2.24	0.00	3.74	10.83	0.45	102.78	5.84	0.11	0.02	6.29	1.03	1.39	0.03	0.29	0.19	0.70	0.00	0.11
HT8-17	35.35	0.80	31.95	0.00	11.14	4.73	0.84	0.30	2.38	0.09	3.64	10.55	0.20	101.96	5.83	0.10	0.00	6.21	1.54	1.16	0.04	0.13	0.15	0.76	0.02	0.07
HT8-18	37.48	0.54	29.74	0.00	5.72	9.23	1.58	0.12	2.26	0.02	3.71	10.76	0.40	101.57	6.05	0.07	0.00	5.66	0.77	2.22	0.02	0.26	0.27	0.71	0.00	0.01
HT8-19	33.97	0.61	34.17	0.00	15.24	0.74	0.40	0.10	2.22	0.05	3.58	10.38	0.23	101.69	5.69	0.08	0.00	6.75	2.13	0.18	0.01	0.15	0.07	0.72	0.01	0.20
HT8-20	34.58	0.26	33.68	0.01	14.45	1.15	0.21	0.24	2.07	0.08	3.57	10.34	0.19	100.83	5.81	0.03	0.00	6.67	2.03	0.29	0.03	0.13	0.04	0.67	0.02	0.27
HT8-21	37.52	0.35	31.40	0.06	6.77	7.45	0.02	0.00	2.86	0.00	3.71	10.75	0.39	101.27	6.07	0.04	0.01	5.98	0.92	1.80	0.00	0.25	0.00	0.90	0.00	0.10
HT8-22	36.69	0.61	32.60	0.05	7.32	6.44	0.53	0.10	2.52	0.00	3.71	10.74	0.33	101.64	5.93	0.07	0.01	6.21	0.99	1.55	0.01	0.21	0.09	0.79	0.00	0.12
HT8-23	36.13	0.75	25.00	0.41	11.79	9.31	2.07	0.02	2.11	0.04	3.58	10.37	0.00	101.57	6.06	0.09	0.05	4.94	1.65	2.33	0.00	0.00	0.37	0.69	0.01	0.00
HT8-24	36.56	1.35	30.86		8.46	6.53	0.91	0.12	2.16	0.07	3.68	10.66	0.29	101.65	5.96	0.17	0.00	5.93	1.15	1.59	0.02	0.19	0.16	0.68	0.01	0.14
HT8-25	37.89	0.59	32.10	0.04	3.75	9.50	0.74	0.03	2.70	0.09	3.79	10.99	0.33	102.54	5.99	0.07	0.01	5.98	0.50	2.24	0.00	0.21	0.13	0.83	0.02	0.03

样品号	主量元素(%)												原子数(个)													
	SiO <sub>2</sub>	TiO <sub>2</sub>	Al <sub>2</sub> O <sub>3</sub>	Cr <sub>2</sub> O <sub>3</sub>	FeO	MgO	CaO	MnO	Na <sub>2</sub> O	K <sub>2</sub> O	H <sub>2</sub> O*	B <sub>2</sub> O <sub>3</sub> *	Li <sub>2</sub> O*	Total	Si	Ti	Cr	Al	Fe <sup>2+</sup>	Mg	Mn	Li*	Ca	Na	K	γ
HT8-26	35.88	0.70	32.37	0.42	9.22	5.08	0.50	0.15	2.26	0.06	3.65	10.59	0.27	101.15	5.89	0.09	0.05	6.26	1.27	1.24	0.02	0.18	0.09	0.72	0.01	0.18
HT8-27	37.35	0.65	32.64	0.07	6.15	7.22	0.22	0.03	2.51	0.00	3.74	10.83	0.29	101.69	5.99	0.08	0.01	6.17	0.83	1.73	0.00	0.19	0.04	0.78	0.00	0.18
HT8-28	35.17	0.91	32.73	0.06	10.24	4.96	1.34	0.00	1.94	0.15	3.66	10.61	0.29	102.06	5.76	0.11	0.01	6.32	1.40	1.21	0.00	0.19	0.24	0.62	0.03	0.12
HT8-29	34.56	0.91	31.65	0.00	15.33	1.95	0.71	0.00	2.27	0.00	3.56	10.33	0.21	101.48	5.82	0.12	0.00	6.28	2.16	0.49	0.00	0.14	0.13	0.74	0.00	0.13
HT8-30	37.01	0.71	31.30	0.09	10.30	5.91	0.07	0.05	2.58	0.00	3.69	10.70	0.11	102.51	6.01	0.09	0.01	5.99	1.40	1.43	0.01	0.07	0.01	0.81	0.00	0.18
HT8-31	36.03	1.07	33.88	0.21	7.15	5.77	0.82	0.00	1.99	0.11	3.72	10.79	0.40	101.94	5.80	0.13	0.03	6.43	0.96	1.39	0.00	0.26	0.14	0.62	0.02	0.21
HT8-32	36.74	0.50	33.69	0.06	7.30	6.06	0.86	0.00	2.28	0.00	3.74	10.85	0.41	102.49	5.89	0.06	0.01	6.36	0.98	1.45	0.00	0.26	0.15	0.71	0.00	0.14
HT8-33	35.50	0.40	31.97	0.00	14.59	1.69	0.01	0.26	2.35	0.00	3.57	10.34	0.20	100.88	5.97	0.05	0.00	6.33	2.05	0.42	0.04	0.14	0.00	0.77	0.00	0.23

注:H<sub>2</sub>O\*、B<sub>2</sub>O<sub>3</sub>\*和Li<sub>2</sub>O\*表示电子探针无法直接测得其含量,主要根据电气石的标准化学组成反算获得,Li<sup>+</sup>\*原子数是根据反算的Li<sub>2</sub>O\*含量计算而得,γ原子数表示阳离子空位原子数,电气石(XY<sub>3</sub>Z<sub>6</sub>(T<sub>6</sub>O<sub>8</sub>)(BO<sub>3</sub>)<sub>3</sub>V<sub>3</sub>W)X位阳离子包括Na<sup>+</sup>、Ca<sup>2+</sup>和阳离子空位γ。

表2 扬子克拉通西缘下三叠统飞仙关组(HT1)和上三叠统须家河组(HT8)砂岩铬尖晶石电子探针数据表

Annexed Table 2 Chromian spinel electron probe data of the Lower Triassic Feixianguan Formation (HT1) and the Upper Triassic Xujiache Formation (HT8) on the western margin of the Yangtze Craton

样品号	主量元素(%)												原子数(个)												Mg <sup>#</sup>	Cr <sup>#</sup>
	SiO <sub>2</sub>	TiO <sub>2</sub>	Al <sub>2</sub> O <sub>3</sub>	Cr <sub>2</sub> O <sub>3</sub>	FeO*	MnO	MgO	NiO	CaO	Total	FeO	Fe <sub>2</sub> O <sub>3</sub>	Si	Ti	Al	Cr	Fe <sup>3+</sup>	Fe <sup>2+</sup>	Mn	Mg	Ni					
飞仙关组样品(HT1)																										
HT1-2	0.17	4.12	8.51	42.48	36.27	0.27	7.88	0.04	0.00	99.74	25.12	12.39	0.01	0.10	0.34	1.13	0.31	0.71	0.01	0.39	0.00	0.36	0.77			
HT1-3	0.12	2.63	13.27	43.82	29.77	0.25	9.56	0.13	0.02	99.57	21.68	8.99	0.00	0.06	0.51	1.13	0.22	0.59	0.01	0.47	0.00	0.44	0.69			
HT1-4	0.14	1.50	8.12	50.59	31.46	0.42	6.86	0.24	0.00	99.32	23.67	8.66	0.00	0.04	0.33	1.36	0.22	0.68	0.01	0.35	0.01	0.34	0.81			
HT1-5	0.18	1.77	15.54	42.34	29.02	0.30	10.31	0.16	0.03	99.65	20.15	9.87	0.01	0.04	0.59	1.08	0.24	0.54	0.01	0.49	0.00	0.48	0.65			
HT1-6	0.18	1.83	12.30	47.73	26.53	0.24	10.93	0.27	0.02	100.03	18.81	8.58	0.01	0.04	0.47	1.22	0.21	0.51	0.01	0.53	0.01	0.51	0.72			
HT1-7	0.21	0.79	15.57	46.45	27.29	0.34	7.93	0.16	0.00	98.73	22.57	5.24	0.01	0.02	0.61	1.21	0.13	0.62	0.01	0.39	0.00	0.39	0.67			
HT1-8	0.11	2.30	11.12	45.31	31.00	0.33	8.57	0.17	0.02	98.93	22.23	9.74	0.00	0.06	0.44	1.20	0.24	0.62	0.01	0.43	0.00	0.41	0.73			
HT1-9	0.05	1.26	20.07	39.25	28.09	0.31	9.21	0.09	0.00	98.33	21.54	7.27	0.00	0.03	0.76	1.00	0.18	0.58	0.01	0.44	0.00	0.43	0.57			
HT1-10	0.16	1.71	13.86	44.90	27.07	0.35	11.18	0.16	0.01	99.39	18.36	9.68	0.01	0.04	0.53	1.14	0.23	0.50	0.01	0.54	0.00	0.52	0.68			
HT1-11	0.13	1.79	13.92	46.33	27.23	0.31	8.87	0.21	0.02	98.81	21.67	6.18	0.00	0.04	0.54	1.21	0.15	0.60	0.01	0.44	0.01	0.42	0.69			
HT1-12	0.20	0.96	16.55	47.03	23.61	0.32	10.47	0.11	0.02	99.25	19.19	4.91	0.01	0.02	0.63	1.20	0.12	0.52	0.01	0.50	0.00	0.49	0.66			
HT1-13	0.13	1.76	12.37	48.57	25.57	0.32	11.43	0.17	0.02	100.34	18.04	8.37	0.00	0.04	0.47	1.24	0.20	0.49	0.01	0.55	0.00	0.53	0.72			
HT1-14	0.15	5.05	7.43	42.30	37.57	0.40	5.37	0.09	0.01	98.37	28.92	9.61	0.01	0.13	0.31	1.17	0.25	0.84	0.01	0.28	0.00	0.25	0.79			
HT1-15	0.13	2.42	11.36	47.13	28.32	0.36	10.07	0.06	0.02	99.88	20.47	8.72	0.00	0.06	0.44	1.22	0.21	0.56	0.01	0.49	0.00	0.47	0.74			
HT1-17	0.10	1.96	11.63	45.70	30.40	0.34	8.95	0.24	0.02	99.33	21.47	9.93	0.00	0.05	0.45	1.20	0.25	0.59	0.01	0.44	0.01	0.43	0.73			
HT1-18	0.16	1.97	11.71	44.75	31.65	0.35	8.75	0.29	0.02	99.65	21.94	10.78	0.01	0.05	0.46	1.17	0.27	0.61	0.01	0.43	0.01	0.42	0.72			

样品号	主量元素(%)												原子数(个)										Mg <sup>#</sup>	Cr <sup>#</sup>
	SiO <sub>2</sub>	TiO <sub>2</sub>	Al <sub>2</sub> O <sub>3</sub>	Cr <sub>2</sub> O <sub>3</sub>	FeO <sup>*</sup>	MnO	MgO	NiO	CaO	Total	FeO	Fe <sub>2</sub> O <sub>3</sub>	Si	Ti	Al	Cr	Fe <sup>3+</sup>	Fe <sup>2+</sup>	Mn	Mg	Ni			
HT1-20	0.09	1.69	11.89	48.74	25.50	0.35	10.71	0.16	0.01	99.15	18.54	7.74	0.00	0.04	0.46	1.26	0.19	0.51	0.01	0.52	0.00	0.51	0.73	
HT1-21	0.11	2.14	12.31	45.87	27.54	0.44	10.74	0.23	0.03	99.40	18.93	9.57	0.00	0.05	0.47	1.18	0.23	0.52	0.01	0.52	0.01	0.50	0.71	
HT1-22	0.10	1.72	12.60	44.08	35.94	0.39	4.37	0.09	0.00	99.29	28.51	8.26	0.00	0.04	0.51	1.19	0.21	0.81	0.01	0.22	0.00	0.21	0.70	
HT1-23	0.06	3.39	11.30	39.98	36.55	0.44	8.14	0.06	0.00	99.92	24.24	13.68	0.00	0.08	0.44	1.05	0.34	0.67	0.01	0.40	0.00	0.37	0.70	
HT1-24	0.11	1.73	10.94	47.06	30.34	0.37	8.75	0.16	0.00	99.46	21.58	9.74	0.00	0.04	0.43	1.24	0.24	0.60	0.01	0.43	0.00	0.42	0.74	
HT1-25	0.21	1.91	9.87	48.78	28.91	0.33	8.68	0.10	0.01	98.80	21.66	8.06	0.01	0.05	0.39	1.30	0.20	0.61	0.01	0.43	0.00	0.42	0.77	
HT1-26	0.21	1.62	12.50	46.64	26.64	0.33	11.19	0.28	0.00	99.40	18.01	9.59	0.01	0.04	0.48	1.20	0.23	0.49	0.01	0.54	0.01	0.53	0.71	
HT1-27	0.06	1.93	13.25	45.78	30.25	0.29	8.88	0.18	0.00	100.60	22.27	8.86	0.00	0.05	0.51	1.18	0.22	0.61	0.01	0.43	0.00	0.42	0.70	
HT1-28	0.20	1.82	14.12	45.72	25.45	0.33	11.30	0.30	0.01	99.25	18.17	8.10	0.01	0.04	0.54	1.17	0.20	0.49	0.01	0.54	0.01	0.53	0.68	
HT1-29	0.10	3.61	10.42	43.42	30.54	0.30	10.37	0.25	0.02	99.01	20.55	11.10	0.00	0.09	0.41	1.13	0.28	0.57	0.01	0.51	0.01	0.47	0.74	
HT1-30	0.16	4.66	9.83	44.62	29.99	0.39	9.68	0.32	0.00	99.65	22.56	8.26	0.01	0.12	0.38	1.17	0.21	0.62	0.01	0.48	0.01	0.43	0.75	

须家河组样品(HT8)

HT8-1	0.43	0.08	12.57	55.40	20.09	0.55	9.31	0.00	0.09	98.52	19.29	0.88	0.01	0.00	0.49	1.45	0.02	0.54	0.02	0.46	0.00	0.46	0.75
HT8-4	0.24	0.64	16.70	40.70	29.00	0.19	11.82	0.14	0.02	99.45	17.12	13.21	0.01	0.02	0.62	1.02	0.31	0.45	0.01	0.56	0.00	0.55	0.62
HT8-7	0.37	0.14	3.16	56.44	32.01	0.36	5.65	0.24	0.02	98.39	23.47	9.49	0.01	0.00	0.13	1.58	0.25	0.70	0.01	0.30	0.01	0.30	0.92
HT8-8	0.39	0.31	14.12	49.29	26.17	0.29	8.32	0.23	0.12	99.24	21.47	5.22	0.01	0.01	0.55	1.28	0.13	0.59	0.01	0.41	0.01	0.41	0.70
HT8-9	0.33	2.18	24.16	33.43	28.05	0.56	9.04	0.20	0.05	98.00	22.82	5.81	0.01	0.05	0.90	0.84	0.14	0.60	0.02	0.43	0.01	0.41	0.48
HT8-10	0.49	0.00	6.26	58.57	26.66	0.31	6.19	0.07	0.00	98.55	23.46	3.56	0.02	0.00	0.26	1.62	0.09	0.68	0.01	0.32	0.00	0.32	0.86
HT8-11	0.46	0.21	10.65	48.34	32.75	0.69	5.44	0.17	0.00	98.71	24.77	8.87	0.02	0.01	0.43	1.30	0.23	0.71	0.02	0.28	0.00	0.28	0.75
HT8-13	0.48	0.49	8.41	47.49	34.07	2.59	2.51	0.41	0.05	96.50	25.44	9.60	0.02	0.01	0.35	1.33	0.26	0.75	0.08	0.13	0.01	0.15	0.79
HT8-14	0.36	0.05	8.27	53.36	28.85	0.92	7.04	0.02	0.00	98.87	21.58	8.08	0.01	0.00	0.33	1.43	0.21	0.61	0.03	0.36	0.00	0.37	0.81
HT8-15	0.37	0.22	11.16	58.14	15.24	0.48	12.20	0.11	0.00	97.92	14.61	0.71	0.01	0.01	0.43	1.51	0.02	0.40	0.01	0.60	0.00	0.60	0.78
HT8-16	0.35	0.19	10.76	55.42	21.03	0.67	9.73	0.00	0.06	98.21	17.75	3.64	0.01	0.00	0.42	1.46	0.09	0.49	0.02	0.48	0.00	0.49	0.78
HT8-17	0.56	0.27	10.30	47.34	31.36	0.39	6.39	0.25	0.05	96.91	23.28	8.97	0.02	0.01	0.42	1.29	0.23	0.67	0.01	0.33	0.01	0.33	0.76
HT8-18	0.44	0.23	6.78	59.57	22.79	0.65	7.40	0.00	0.09	97.95	21.22	1.74	0.02	0.01	0.28	1.63	0.05	0.62	0.02	0.38	0.00	0.38	0.85
HT8-21	0.45	1.25	18.06	40.74	25.88	0.32	11.51	0.78	0.03	99.02	17.67	9.12	0.01	0.03	0.67	1.02	0.22	0.47	0.01	0.54	0.02	0.54	0.60
HT8-23	0.42	0.11	10.87	54.28	28.25	0.85	4.62	0.04	0.17	99.61	26.19	2.28	0.01	0.00	0.44	1.47	0.06	0.75	0.02	0.24	0.00	0.24	0.77
HT8-24	0.56	2.51	14.95	41.68	28.42	0.45	9.49	0.10	0.07	98.23	21.74	7.42	0.02	0.06	0.58	1.08	0.18	0.60	0.01	0.46	0.00	0.44	0.65
HT8-25	0.58	0.56	28.42	34.58	19.58	0.25	15.08	0.01	0.00	99.06	14.25	5.92	0.02	0.01	1.00	0.81	0.13	0.35	0.01	0.67	0.00	0.65	0.45
HT8-26	0.41	0.09	12.95	46.33	31.00	0.64	6.78	0.00	0.03	98.23	23.20	8.66	0.01	0.00	0.51	1.23	0.22	0.65	0.02	0.34	0.00	0.34	0.71
HT8-29	0.49	1.01	6.41	49.54	34.88	0.32	5.25	0.35	0.00	98.25	25.19	10.77	0.02	0.03	0.26	1.37	0.28	0.73	0.01	0.27	0.01	0.27	0.84
HT8-30	0.56	0.81	13.32	46.22	27.54	0.58	9.59	0.19	0.00	98.81	19.91	8.48	0.02	0.02	0.52	1.20	0.21	0.55	0.02	0.47	0.01	0.46	0.70

注:FeO<sup>\*</sup> 表示全铁, Fe<sub>2</sub>O<sub>3</sub> 根据尖晶石的化学计量比计算。

附表 3 扬子克拉通西缘下三叠统飞仙关组(HT1)和上三叠统须家河组(HT8)砂岩碎屑锆石 LA-ICP-MS U-Pb 数据表  
 Annexed Table 3 Detrital zircon U-Pb isotopic data from the Lower Triassic Feixianguan Formation (HT1) and the Upper Triassic Xujiahe Formation (HT8) on the western margin of the Yangtze Craton

测点号	元素含量( $\times 10^{-6}$ )			Th/U	同位素比值						同位素年龄(Ma)						谐和度 (%)		
	Pb	Th	U		$n(^{207}\text{Pb})/n(^{206}\text{Pb})$			$n(^{207}\text{Pb})/n(^{235}\text{U})$			$n(^{206}\text{Pb})/n(^{238}\text{U})$			$n(^{207}\text{Pb})/n(^{206}\text{Pb})$					
					测值	1 $\sigma$	测值	1 $\sigma$	测值	1 $\sigma$	测值	1 $\sigma$	测值	1 $\sigma$	测值	1 $\sigma$			
飞仙关组样品(HT1)																			
HT1-2	66	131	530	0.25	0.0657	0.0005	1.1453	0.0162	0.1262	0.0012	798	14	775	8	766	7	101		
HT1-3	90	152	290	0.52	0.1042	0.0007	4.2025	0.0587	0.2922	0.0029	1699	12	1675	11	1652	14	103		
HT1-4	19	94	158	0.59	0.0636	0.0005	1.0391	0.0167	0.1184	0.0012	729	18	723	8	722	7	100		
HT1-5	22	127	131	0.97	0.0706	0.0006	1.4907	0.0228	0.1531	0.0015	946	16	927	9	918	8	101		
HT1-6	10	55	81	0.68	0.0704	0.0008	1.1848	0.0232	0.1218	0.0012	941	23	794	11	741	7	107		
HT1-7	44	84	395	0.21	0.0589	0.0004	0.9644	0.0138	0.1186	0.0012	563	15	686	7	722	7	95		
HT1-8	40	276	347	0.80	0.0630	0.0004	1.0200	0.0147	0.1174	0.0011	707	15	714	7	715	7	100		
HT1-9	36	233	319	0.73	0.0621	0.0005	0.9837	0.0144	0.1148	0.0011	676	15	695	7	701	7	99		
HT1-10	17	94	134	0.70	0.0647	0.0005	1.1048	0.0172	0.1238	0.0012	763	16	756	8	752	7	101		
HT1-11	29	668	722	0.93	0.0503	0.0003	0.2718	0.0023	0.0392	0.0001	211	15	244	2	247.6	0.6	99		
HT1-12	33	175	242	0.72	0.0657	0.0005	1.1505	0.0168	0.1269	0.0012	796	15	777	8	770	7	101		
HT1-13	8	52	61	0.84	0.0641	0.0010	1.0367	0.0247	0.1171	0.0012	744	32	722	12	714	7	101		
HT1-14	27	282	291	0.97	0.0590	0.0005	0.7044	0.0109	0.0866	0.0008	567	17	541	7	535	5	101		
HT1-15	10	151	229	0.66	0.0550	0.0009	0.2953	0.0070	0.0388	0.0004	414	34	263	5	246	2	107		
HT1-16	3	45	59	0.76	0.0547	0.0040	0.3049	0.0255	0.0401	0.0005	400	165	270	20	253	3	107		
HT1-18	23	373	187	1.99	0.0580	0.0006	0.6169	0.0116	0.0771	0.0008	531	23	488	7	479	5	102		
HT1-19	52	151	105	1.44	0.1291	0.0009	6.3827	0.0895	0.3588	0.0035	2085	12	2030	12	1976	17	106		
HT1-20	30	163	282	0.58	0.0622	0.0005	0.8535	0.0127	0.0995	0.0010	681	15	627	7	612	6	102		
HT1-21	205	301	385	0.78	0.1670	0.0011	10.2169	0.1431	0.4438	0.0044	2528	11	2455	13	2368	20	107		
HT1-22	178	164	371	0.44	0.1651	0.0011	9.8454	0.1375	0.4326	0.0043	2508	11	2420	13	2317	19	108		
HT1-23	14	137	88	1.56	0.0663	0.0008	1.1482	0.0236	0.1257	0.0013	816	25	776	11	763	7	102		
HT1-24	18	98	130	0.76	0.0649	0.0006	1.1371	0.0187	0.1270	0.0013	772	18	771	9	771	7	100		
HT1-25	73	230	385	0.60	0.0784	0.0005	1.9242	0.0270	0.1780	0.0017	1158	13	1090	9	1056	10	110		
HT1-26	8	126	176	0.72	0.0531	0.0015	0.2906	0.0109	0.0397	0.0004	331	65	259	9	251	2	103		
HT1-27	16	194	158	1.22	0.0598	0.0007	0.6981	0.0135	0.0848	0.0008	594	24	538	8	525	5	102		
HT1-28	28	104	304	0.34	0.0657	0.0009	0.7974	0.0179	0.0881	0.0009	796	27	595	10	544	5	109		
HT1-30	18	113	122	0.93	0.0741	0.0007	1.2700	0.0213	0.1242	0.0012	1045	18	832	10	754	7	110		
HT1-31	2	32	34	0.96	0.0491	0.0061	0.3010	0.0410	0.0419	0.0006	152	257	267	32	265	3	101		
HT1-32	7	210	139	1.51	0.0523	0.0016	0.2689	0.0104	0.0372	0.0004	299	68	242	8	235	2	103		

测点号	元素含量( $\times 10^{-6}$ )			Th/U	同位素比值						同位素年龄(Ma)						谐和度 (%)		
	Pb	Th	U		$n(^{207}\text{Pb})/n(^{206}\text{Pb})$		$n(^{207}\text{Pb})/n(^{235}\text{U})$		$n(^{206}\text{Pb})/n(^{238}\text{U})$		$n(^{207}\text{Pb})/n(^{206}\text{Pb})$		$n(^{207}\text{Pb})/n(^{235}\text{U})$		$n(^{206}\text{Pb})/n(^{238}\text{U})$				
					测值	1 $\sigma$	测值	1 $\sigma$	测值	1 $\sigma$	测值	1 $\sigma$	测值	1 $\sigma$	测值	1 $\sigma$			
HT1-33	21	60	223	0.27	0.0604	0.0005	0.7888	0.0131	0.0948	0.0010	616	18	590	7	584	6	101		
HT1-34	8	30	94	0.33	0.0588	0.0010	0.6791	0.0176	0.0838	0.0008	558	38	526	11	519	5	101		
HT1-35	36	180	277	0.65	0.0638	0.0005	1.0527	0.0156	0.1197	0.0012	735	15	730	8	729	7	100		
HT1-36	18	76	163	0.47	0.0616	0.0006	0.9196	0.0154	0.1084	0.0011	659	19	662	8	663	6	100		
HT1-37	55	1178	1262	0.93	0.0481	0.0002	0.2526	0.0015	0.0381	0.0001	103	9	229	1	240.8	0.5	95		
HT1-38	7	99	177	0.56	0.0494	0.0011	0.2669	0.0065	0.0391	0.0001	167	49	240	5	247.3	0.6	97		
HT1-39	21	85	128	0.67	0.0702	0.0012	1.3951	0.0364	0.1442	0.0015	933	34	887	15	868	8	102		
HT1-41	31	170	166	1.02	0.0706	0.0006	1.4951	0.0231	0.1537	0.0015	945	16	928	9	921	8	101		
HT1-42	59	85	179	0.47	0.1052	0.0010	4.3897	0.0795	0.3026	0.0030	1718	17	1710	15	1704	15	101		
HT1-43	24	187	152	1.23	0.0643	0.0006	1.0937	0.0177	0.1233	0.0012	753	18	750	9	750	7	100		
HT1-46	33	175	174	1.01	0.0723	0.0005	1.5759	0.0235	0.1580	0.0015	995	15	961	9	946	9	102		
HT1-47	65	105	446	0.24	0.0688	0.0005	1.3843	0.0194	0.1460	0.0014	892	14	882	8	878	8	100		
HT1-48	7	115	69	1.67	0.0580	0.0014	0.6457	0.0216	0.0806	0.0008	531	54	506	13	500	5	101		
HT1-49	34	151	249	0.61	0.0660	0.0005	1.1471	0.0171	0.1260	0.0013	808	15	776	8	765	7	101		
HT1-50	89	127	217	0.59	0.1360	0.0009	6.9290	0.0962	0.3695	0.0036	2177	11	2102	12	2027	17	107		
HT1-51	7	98	166	0.59	0.0515	0.0015	0.2869	0.0107	0.0404	0.0004	264	66	256	8	255	2	100		
HT1-53	335	1072	1071	1.00	0.0979	0.0007	3.5125	0.0491	0.2602	0.0026	1585	12	1530	11	1491	13	106		
HT1-54	48	117	482	0.24	0.0616	0.0004	0.8575	0.0123	0.1011	0.0010	659	15	629	7	621	6	101		
HT1-57	9	161	205	0.79	0.0601	0.0012	0.6682	0.0147	0.0803	0.0002	609	40	520	9	498	1	104		
HT1-58	25	89	257	0.34	0.0599	0.0005	0.8031	0.0121	0.0973	0.0010	599	16	599	7	598	6	100		
HT1-59	39	155	288	0.54	0.0654	0.0005	1.1677	0.0168	0.1295	0.0013	786	15	786	8	785	7	100		
HT1-60	63	152	402	0.38	0.0705	0.0005	1.5022	0.0212	0.1544	0.0015	944	14	931	9	926	8	101		
HT1-61	47	141	79	1.78	0.1580	0.0011	9.3975	0.1322	0.4312	0.0042	2435	11	2378	13	2311	19	105		
HT1-62	52	337	780	0.43	0.0550	0.0004	0.4984	0.0074	0.0657	0.0007	414	16	411	5	410	4	100		
HT1-63	22	141	200	0.71	0.0603	0.0005	0.8248	0.0138	0.0992	0.0010	614	19	611	8	610	6	100		
HT1-64	16	263	132	1.99	0.0585	0.0008	0.6964	0.0148	0.0864	0.0009	547	28	537	9	534	5	101		
HT1-65	3	59	68	0.87	0.0627	0.0033	0.7289	0.0418	0.0837	0.0005	697	99	556	25	518	3	107		
HT1-67	194	264	389	0.68	0.1636	0.0011	9.9872	0.1396	0.4427	0.0044	2494	11	2434	13	2363	19	106		
HT1-68	14	91	114	0.79	0.0645	0.0006	1.0554	0.0184	0.1187	0.0012	757	20	732	9	723	7	101		
HT1-69	97	350	562	0.62	0.0751	0.0005	1.7135	0.0250	0.1655	0.0018	1071	14	1014	9	987	10	109		
HT1-70	68	182	674	0.27	0.0622	0.0004	0.8962	0.0126	0.1046	0.0010	679	14	650	7	641	6	101		
HT1-73	52	205	345	0.59	0.0694	0.0005	1.4034	0.0197	0.1467	0.0014	910	14	890	8	882	8	101		
HT1-74	37	714	389	1.84	0.0570	0.0004	0.6158	0.0093	0.0783	0.0008	493	17	487	6	486	5	100		
HT1-76	11	175	276	0.63	0.0591	0.0007	0.9827	0.0129	0.1205	0.0002	569	25	695	7	734	1	95		

测点号	元素含量( $\times 10^{-6}$ )			Th/U	同位素比值						同位素年龄(Ma)							
	Pb	Th	U		$n(^{207}\text{Pb})/n(^{206}\text{Pb})$		$n(^{207}\text{Pb})/n(^{235}\text{U})$		$n(^{206}\text{Pb})/n(^{238}\text{U})$		$n(^{207}\text{Pb})/n(^{206}\text{Pb})$		$n(^{207}\text{Pb})/n(^{235}\text{U})$		$n(^{206}\text{Pb})/n(^{238}\text{U})$		谐和度 (%)	
					测值	1 $\sigma$	测值	1 $\sigma$	测值	1 $\sigma$	测值	1 $\sigma$	测值	1 $\sigma$	测值	1 $\sigma$		
HT1-77	7	148	179	0.83	0.0532	0.0013	0.2420	0.0078	0.0330	0.0003	338	53	220	6	209	2	105	
HT1-79	6	143	139	1.02	0.0602	0.0017	0.6149	0.0187	0.0740	0.0002	611	62	487	12	460	1	106	
HT1-80	6	31	46	0.67	0.0654	0.0014	1.1490	0.0350	0.1274	0.0013	786	46	777	17	773	7	101	
HT1-81	30	315	207	1.52	0.0636	0.0005	0.9905	0.0154	0.1130	0.0011	727	17	699	8	690	6	101	
HT1-83	112	117	235	0.50	0.1646	0.0011	9.7138	0.1361	0.4281	0.0042	2503	11	2408	13	2297	19	109	
HT1-85	36	194	359	0.54	0.0602	0.0005	0.8049	0.0122	0.0969	0.0010	612	16	600	7	596	6	101	
HT1-86	114	31	853	0.04	0.0697	0.0005	1.3709	0.0190	0.1427	0.0014	918	13	877	8	860	8	102	
HT1-87	47	161	370	0.44	0.0652	0.0005	1.1240	0.0161	0.1251	0.0012	780	13	765	8	760	7	101	
HT1-88	17	275	437	0.63	0.0638	0.0004	1.0178	0.0092	0.1157	0.0003	734	15	713	5	706	2	101	

须家河组样品(HT8)

HT8-01	6	60	101	0.59	0.0514	0.0020	0.2946	0.0153	0.0416	0.0006	257	92	262	12	263	4	100
HT8-02	22	6	272	0.02	0.0554	0.0009	0.5412	0.0136	0.0709	0.0008	427	36	439	9	442	5	99
HT8-03	87	84	126	0.67	0.1608	0.0009	10.3251	0.1269	0.4656	0.0050	2464	9	2464	11	2464	22	100
HT8-04	20	146	162	0.90	0.0580	0.0010	0.6768	0.0181	0.0846	0.0010	531	38	525	11	523	6	100
HT8-05	98	89	222	0.40	0.1137	0.0006	5.2426	0.0659	0.3344	0.0035	1859	10	1860	11	1860	17	100
HT8-06	18	111	96	1.15	0.0646	0.0011	1.1065	0.0310	0.1243	0.0016	760	38	757	15	755	9	100
HT8-07	9	33	52	0.63	0.0663	0.0015	1.2279	0.0428	0.1343	0.0019	815	49	813	19	813	11	100
HT8-08	51	382	1004	0.38	0.0526	0.0013	0.3258	0.0113	0.0449	0.0006	312	56	286	9	283	3	101
HT8-09	16	143	143	1.00	0.0564	0.0010	0.5805	0.0165	0.0747	0.0009	467	41	465	11	464	5	100
HT8-10	17	176	283	0.62	0.0517	0.0010	0.3186	0.0090	0.0447	0.0005	271	43	281	7	282	3	100
HT8-11	10	49	59	0.84	0.0645	0.0014	1.1161	0.0372	0.1254	0.0017	759	47	761	18	762	10	100
HT8-12	20	87	96	0.91	0.0685	0.0011	1.3494	0.0344	0.1428	0.0018	885	33	867	15	860	10	101
HT8-13	13	37	70	0.52	0.0680	0.0013	1.3501	0.0409	0.1439	0.0019	869	41	868	18	867	11	100
HT8-14	5	36	59	0.61	0.0547	0.0023	0.4488	0.0249	0.0595	0.0010	400	94	376	17	373	6	101
HT8-15	14	128	62	2.07	0.0636	0.0013	1.0945	0.0335	0.1249	0.0016	727	43	751	16	758	9	99
HT8-17	10	69	193	0.36	0.0513	0.0012	0.2994	0.0104	0.0423	0.0005	256	56	266	8	267	3	100
HT8-18	53	64	128	0.50	0.1132	0.0012	5.1892	0.1056	0.3324	0.0044	1852	19	1851	17	1850	21	100
HT8-19	34	376	349	1.08	0.0606	0.0022	0.5069	0.0240	0.0606	0.0008	626	80	416	16	379	5	110
HT8-20	37	24	87	0.27	0.1132	0.0008	5.2017	0.0820	0.3331	0.0038	1852	14	1853	13	1853	18	100
HT8-21	121	109	262	0.42	0.1139	0.0006	5.2575	0.0628	0.3348	0.0035	1862	10	1862	10	1862	17	100
HT8-22	15	89	216	0.41	0.0514	0.0019	0.2858	0.0140	0.0403	0.0006	258	85	255	11	255	4	100
HT8-23	85	61	192	0.31	0.1126	0.0006	5.1347	0.0652	0.3306	0.0035	1842	10	1842	11	1841	17	100
HT8-24	134	150	185	0.81	0.1625	0.0009	10.5253	0.1275	0.4697	0.0050	2482	9	2482	11	2482	22	100
HT8-25	10	36	57	0.63	0.0668	0.0022	1.2509	0.0602	0.1358	0.0024	832	71	824	27	821	14	100

测点号	元素含量( $\times 10^{-6}$ )			Th/U	同位素比值						同位素年龄(Ma)							
	Pb	Th	U		$n(^{207}\text{Pb})/n(^{206}\text{Pb})$		$n(^{207}\text{Pb})/n(^{235}\text{U})$		$n(^{206}\text{Pb})/n(^{238}\text{U})$		$n(^{207}\text{Pb})/n(^{206}\text{Pb})$		$n(^{207}\text{Pb})/n(^{235}\text{U})$		$n(^{206}\text{Pb})/n(^{238}\text{U})$		谐和度 (%)	
					测值	1 $\sigma$	测值	1 $\sigma$	测值	1 $\sigma$	测值	1 $\sigma$	测值	1 $\sigma$	测值	1 $\sigma$		
HT8-26	3	16	16	1.03	0.0659	0.0040	1.2050	0.0993	0.1326	0.0034	803	129	803	46	803	20	100	
HT8-27	14	71	155	0.46	0.0566	0.0013	0.5944	0.0206	0.0762	0.0010	475	53	474	13	473	6	100	
HT8-28	7	69	135	0.51	0.0509	0.0018	0.2637	0.0128	0.0375	0.0006	238	85	238	10	238	3	100	
HT8-29	18	102	179	0.57	0.0572	0.0011	0.6357	0.0186	0.0806	0.0010	499	43	500	12	500	6	100	
HT8-30	40	102	110	0.93	0.0901	0.0008	3.0820	0.0518	0.2480	0.0028	1428	16	1428	13	1428	14	100	
HT8-31	15	201	283	0.71	0.0508	0.0013	0.2630	0.0094	0.0376	0.0005	231	58	237	8	238	3	100	
HT8-32	10	77	186	0.41	0.0514	0.0015	0.2950	0.0117	0.0416	0.0006	259	67	262	9	263	3	100	
HT8-33	14	40	24	1.65	0.1134	0.0016	5.1952	0.1367	0.3324	0.0050	1854	26	1852	22	1850	24	100	
HT8-34	7	17	44	0.40	0.0650	0.0017	1.1319	0.0437	0.1264	0.0019	773	56	769	21	767	11	100	
HT8-35	90	95	201	0.47	0.1150	0.0007	5.3736	0.0696	0.3389	0.0036	1880	11	1881	11	1881	17	100	
HT8-36	42	36	80	0.45	0.1232	0.0014	6.2155	0.1368	0.3657	0.0051	2004	20	2007	19	2009	24	100	
HT8-37	18	94	120	0.78	0.0621	0.0010	0.9502	0.0251	0.1110	0.0013	677	36	678	13	678	8	100	
HT8-38	166	148	409	0.36	0.1122	0.0006	5.0878	0.0660	0.3289	0.0035	1835	11	1834	11	1833	17	100	
HT8-40	7	24	45	0.53	0.0667	0.0023	1.2440	0.0624	0.1353	0.0025	827	74	821	28	818	14	100	
HT8-41	17	12	24	0.48	0.1623	0.0016	10.4960	0.2170	0.4689	0.0068	2480	17	2480	19	2479	30	100	
HT8-42	54	125	153	0.82	0.0890	0.0006	2.9900	0.0453	0.2436	0.0027	1404	14	1405	12	1405	14	100	
HT8-43	70	62	101	0.61	0.1637	0.0009	10.6727	0.1358	0.4728	0.0052	2494	10	2495	12	2496	23	100	
HT8-44	14	175	249	0.70	0.0546	0.0012	0.3258	0.0107	0.0433	0.0006	394	51	286	8	273	3	105	
HT8-45	24	408	376	1.09	0.0520	0.0008	0.3197	0.0082	0.0446	0.0005	284	38	282	6	281	3	100	
HT8-46	43	56	206	0.27	0.0709	0.0006	1.6788	0.0290	0.1718	0.0019	954	18	1001	11	1022	10	93	
HT8-47	165	131	407	0.32	0.1142	0.0006	5.2902	0.0649	0.3359	0.0035	1867	10	1867	10	1867	17	100	
HT8-48	37	57	77	0.73	0.1140	0.0009	5.2735	0.0891	0.3355	0.0040	1864	15	1865	14	1865	19	100	
HT8-49	26	62	51	1.21	0.1197	0.0014	5.8272	0.1283	0.3531	0.0049	1951	21	1950	19	1949	23	100	
HT8-50	42	79	511	0.15	0.0556	0.0006	0.5344	0.0104	0.0697	0.0008	435	24	435	7	435	5	100	
HT8-51	14	69	88	0.78	0.0630	0.0013	1.0126	0.0322	0.1165	0.0015	709	45	710	16	711	9	100	
HT8-52	8	72	57	1.26	0.0592	0.0026	0.7601	0.0458	0.0930	0.0017	576	98	574	26	573	10	100	
HT8-53	16	165	123	1.35	0.0578	0.0011	0.6459	0.0194	0.0810	0.0010	522	44	506	12	502	6	101	
HT8-54	41	55	103	0.53	0.1059	0.0010	4.4960	0.0861	0.3079	0.0038	1730	17	1730	16	1730	19	100	
HT8-55	12	67	71	0.94	0.0687	0.0018	1.2400	0.0476	0.1309	0.0020	890	52	819	22	793	11	103	
HT8-56	18	129	170	0.76	0.0569	0.0010	0.6253	0.0176	0.0798	0.0010	486	39	493	11	495	6	100	
HT8-57	9	50	94	0.53	0.0563	0.0014	0.5790	0.0214	0.0746	0.0010	464	55	464	14	464	6	100	
HT8-58	41	406	505	0.80	0.0540	0.0006	0.4445	0.0088	0.0597	0.0007	370	25	373	6	374	4	100	
HT8-59	11	59	61	0.97	0.0643	0.0014	1.1060	0.0365	0.1247	0.0017	752	45	756	18	758	10	100	
HT8-60	4	56	63	0.89	0.0527	0.0027	0.3603	0.0236	0.0496	0.0009	314	112	312	18	312	5	100	

测点号	元素含量( $\times 10^{-6}$ )			Th/U	同位素比值						同位素年龄(Ma)							
	Pb	Th	U		$n(^{207}\text{Pb})/n(^{206}\text{Pb})$		$n(^{207}\text{Pb})/n(^{235}\text{U})$		$n(^{206}\text{Pb})/n(^{238}\text{U})$		$n(^{207}\text{Pb})/n(^{206}\text{Pb})$		$n(^{207}\text{Pb})/n(^{235}\text{U})$		$n(^{206}\text{Pb})/n(^{238}\text{U})$		谐和度 (%)	
					测值	$1\sigma$	测值	$1\sigma$	测值	$1\sigma$	测值	$1\sigma$	测值	$1\sigma$	测值	$1\sigma$		
HT8-61	70	95	156	0.61	0.1125	0.0007	5.1279	0.0708	0.3305	0.0036	1840	11	1841	12	1841	17	100	
HT8-62	14	20	35	0.57	0.1053	0.0014	4.4409	0.1081	0.3058	0.0043	1720	24	1720	20	1720	21	100	
HT8-63	7	68	102	0.67	0.0534	0.0021	0.4054	0.0214	0.0550	0.0009	348	87	346	15	345	5	100	
HT8-64	6	33	69	0.48	0.0554	0.0023	0.5258	0.0298	0.0688	0.0012	430	92	429	20	429	7	100	
HT8-65	9	48	50	0.95	0.0643	0.0027	1.1128	0.0645	0.1254	0.0025	753	85	760	31	762	14	100	
HT8-66	14	164	275	0.60	0.0515	0.0018	0.2926	0.0142	0.0412	0.0006	261	80	261	11	261	4	100	
HT8-67	5	36	28	1.28	0.0630	0.0026	1.0147	0.0571	0.1167	0.0021	710	86	711	29	712	12	100	
HT8-68	18	129	312	0.41	0.0527	0.0010	0.3685	0.0109	0.0507	0.0006	318	44	319	8	319	4	100	
HT8-69	5	104	90	1.16	0.0518	0.0034	0.2839	0.0235	0.0398	0.0008	277	144	254	19	251	5	101	
HT8-70	30	23	68	0.33	0.1202	0.0012	5.8749	0.1191	0.3545	0.0047	1959	18	1958	18	1956	22	100	
HT8-71	11	146	248	0.59	0.0505	0.0020	0.2506	0.0128	0.0360	0.0005	219	88	227	10	228	3	100	
HT8-72	39	121	205	0.59	0.0684	0.0008	1.3784	0.0292	0.1461	0.0017	881	24	880	12	879	10	100	
HT8-73	34	89	69	1.29	0.1107	0.0012	4.9486	0.1055	0.3242	0.0043	1811	20	1811	18	1810	21	100	
HT8-74	13	81	96	0.84	0.0606	0.0013	0.8516	0.0271	0.1019	0.0013	625	44	626	15	626	8	100	
HT8-75	80	134	169	0.79	0.1129	0.0007	5.1634	0.0688	0.3316	0.0036	1847	11	1847	11	1846	17	100	
HT8-76	4	34	69	0.49	0.0515	0.0024	0.2975	0.0183	0.0419	0.0007	264	106	264	14	264	4	100	
HT8-77	12	53	66	0.80	0.0648	0.0012	1.1357	0.0339	0.1271	0.0017	769	39	770	16	771	9	100	
HT8-78	164	80	259	0.31	0.1800	0.0010	12.5995	0.1625	0.5076	0.0057	2653	9	2650	12	2646	24	100	
HT8-79	25	348	248	1.40	0.0544	0.0012	0.4642	0.0150	0.0619	0.0008	386	48	387	10	387	5	100	
HT8-80	33	60	48	1.23	0.1598	0.0017	10.1551	0.2215	0.4609	0.0070	2453	17	2449	20	2444	31	100	
HT8-81	2	30	44	0.68	0.0511	0.0039	0.2776	0.0258	0.0394	0.0008	247	167	249	21	249	5	100	
HT8-82	139	111	364	0.31	0.1145	0.0009	5.3126	0.0853	0.3365	0.0039	1872	13	1871	14	1870	19	100	
HT8-83	21	155	435	0.36	0.0510	0.0010	0.2576	0.0077	0.0367	0.0004	239	45	233	6	232	3	100	
HT8-84	68	56	128	0.44	0.1715	0.0019	11.5946	0.2667	0.4902	0.0082	2573	18	2572	22	2572	35	100	